In-Vivo Imaging of FLK-1-GFP Positive Cells during Development of the Cardiovascular System

Veronica Sanchez

Department of Human Genetics

McGill University, Montreal

December, 2013

A thesis submitted to the Faculty of Graduate and Postdoctoral Studies in partial fulfillment of the requirements of the degree of Master of Science

TABLE OF CONTENTS

ABSTRACT

The mouse *Flk-1* gene encodes for vascular endothelial growth factor receptor 2 (VEGFR-2), the receptor for vascular endothelial growth factor A (VEGF-A). This gene is essential for the development of the vascular system. In the early embryo, *Flk-1* expression marks angioblasts and subsequent endothelial cells. *Flk-1*$^{-/-}$ embryos die at E8.5-9.5 and fail to develop the blood island, endocardium, dorsal aortae, intersomitic vessels, and capillaries. This gene product is required for endothelial cell development as well as for primitive and definitive erythrocyte differentiation. *Flk-1*$^{-/-}$ cells locate to the amnion, where it is not normally expressed. It is accepted that FLK-1 positive cells contribute to the formation of the endocardium as well as the embryonic vasculature and the extraembryonic yolk sac vasculature; however, the origins of these individual populations remain unknown. We hypothesize FLK-1 positive cells contributing to different lineages originate from different areas and behave differently; therefore, the aim of this project is to identify the origins of endothelial progenitors and study their behavior during their contribution to the cardiovascular system.

Live-imaging microscopy analysis allows temporal and spatial observation of natural processes. Using the *Flk-1*-GFP mouse reporter line, heterozygous and homozygous embryos were used to live-image embryos from E7.5 to E8.5. The origins of endothelial cells forming the cardiovascular system were retrospectively identified with the use of software programs. The process of formation was then compared to that of *Flk-1*$^{GFP/GFP}$ mutant embryos.

Live-imaging analysis of embryos during the streak stages showed the appearance of *Flk-1*-GFP+ cells laterally to the primitive streak. These cells then expanded embryonically and extraembryonically. During the head-fold stages, embryos showed a small population of *Flk-1*-GFP positive cells actively migrating from the embryonic-extraembryonic boundary into the embryonic region to form the dorsal aortae. During the migration, the cells aggregated and luminal structures were formed. The embryonic dorsal aortae form as these small luminal structures aggregated, lined laterally to the embryo midline. We also identified that endocardium progenitors originate from a region more anterior than dorsal aortae angioblasts. The majority of *Flk-1*-GFP+ cells in the extraembryonic region become part of the yolk sac vasculature.

Flk-1$^{GFP/GFP}$ embryos appeared normal during the streak stages; however, during the head-fold stages, *Flk-1*-GFP+ cells showed lack of migration and failed to form vascular structures. The cells were located within the amnion, the base of the allantois, the cardiac mesoderm, and the

extraembryonic region. The heart tube formed although the endocardium was absent. These data show the origins and contribution of *Flk-1*-GFP cells during gastrulation. Moreover, *Flk-1* was found to be dispensable for the migration of mesodermal cell from the primitive streak and essential for angioblast migration.

RÉSUMÉ

Le gène murin *Flk-1* code pour le récepteur 2 du facteur de croissance endothélial vasculaire (VEGFR-2), récepteur au facteur de croissance endothélial vasculaire A (VEGF-A). Ce gène est essentiel au développement du syolk sactème cardiovasculaire. Au stade initial du développement de l'embryon, *Flk-1* est exprimé sur les angioblastes, et sur les cellules endothéliales qui en sont issues. Chez les embryons Flk1$^{-/-}$ on constate la mort à E8.5-9.5, et l'absence de développement des îlots vasculaires, de l'endocarde, de l'aorte dorsale, des vaisseaux intersomitiques et des capillaires. Le produit de ce gène est nécessaire au développement des cellules endothéliales, ainsi qu'à la différenciation primitive et définitive des érythrocytes. Les cellules Flk1$^{-/-}$ sont localisées, de manière normale, dans l'amnios. Il est admis que les cellules exprimant Flk-1 contribuent à la formation de l'endocarde, ainsi qu'à la vascularisation de l'embryon et de la vésicule vitelline; cependent, les origines de ces populations cellulaires individuelles restent inconnues. L'hypothèse émise est que les cellules exprimant Flk-1, à l'origine de différentes lignées cellulaires, proviennent de différentes régions et ont un comportement différent; le but de ce projet est donc d'identifier l'origine des progéniteurs endothéliaux et d'étudier leur comportement contributif au développement du système cardiovasculaire.

L'analyse en videomicroscopie permet une observation temporelle et spatiale de processus naturels. Des embryons issus de la lignée murine Flk-1-GFP, hétérozygotes ou homozygotes, ont été observés en videomicroscopie de E7.5 à E8.5 pour visualiser la formation du système cardiovasculaire. Les origines des cellules endothéliales formant le système cardiovasculaire ont été rétrospectivement identifiées à l'aide de logiciels. Le processus de formation a été comparé à celui d'embryons mutés Flk-1$^{GFP/GFP}$.

L'analyse en videomicroscopie des embryons durant les étapes séquentielles du développement a montré que les cellules Flk-1-GFP+ apparaissent latéralement sur la ligne primitive. Ces cellules se répartissent ensuite dans les régions embryonnaires et extra-embryonnaires. Au cours de "head-fold stage" on a observé l'apparition d'une petite population de cellules Flk-1-GFP+, migrant de la frontière entre les régions embryonnaire et extra-embryonnaire dans la région embryonnaire pour former l'aorte dorsale. Durant cette migration, les cellules s'agrègent et initient la formation luminale. L'aorte dorsale embryonnaire se forme à mesure que ces petites

structures luminales s'agrègent et s'alignent dans la région embryonnaire, formant une structure tubulaire distincte. Nous avons également pu identifier que les progéniteurs endocardiaux sont localisés dans une zone plus antérieure que les angioblastes de l'aorte dorsale. La majorité des cellules Flk-1-GFP+ de la région extra-embryonnaire forme la vascularisation de la vésicule vitelline. Les embryons Flk-$1^{GFP/GFP}$ sont apparus normaux au cours des étapes séquentielles, cependant, durant les étapes "head-fold", ni la migration ni les structures vasculaires n'ont été observées. Les cellules ont été localisées à l'intérieur de l'amnios, de l'allantoïde, du mésoderme cardiaque et de la région extra-embryonnaire. Le tube cardiaque s'est formé malgré l'absence de l'endocarde. Ces données montrent les origines des cellules exprimant Flk-1-GFP et leur contribution dans la gastrulation; de plus, il a été montré que Flk-1 est indispensable à la migration des cellules du mésoderme de la ligne primitive ainsi qu'à la migration des angioblastes.

ACKNOWLEDGEMENTS

I thank my supervisor Dr. Yojiro Yamanaka for his unconditional support during my Masters. I would also like to thank the members of my supervisory committee, Dr. Loydie Majewska and Dr. Elizabeth Jones, for encouraging me during my experiments and for letting me get the most out of my graduate education. They were both present and helped me with questions and data analysis. Also, a big thank you to Nobuko Yamanaka, the laboratory technician, for teaching me and aiding me in the care of my mouse colony.

During my project, I started making transgenic lines. Dr. Dayana Krawchuk taught me the molecular aspect of the protocol. From her I was able to acquire a great deal of knowledge that I will take onto my next research project. I am in great debt to her.

More importantly, none of this work could have done without the support of my family and friends: my parents and grandparents, who supported me from thousands of kilometers away, and my friends in Puerto Rico, Ontario, and Quebec, especially the ones in Montreal who stayed with me late into the nights on many occasions.

CONTRIBUTIONS

This project has been written in accordance to the Faculty of Graduate Studies and Post-doctoral Studies' guidelines, at McGill University. Mouse studies have been performed following the regulations of the Canadian council of Animal Care. The candidate was responsible for planning and executing the experiments presented. Data analysis and the writing of the manuscript was done in conjunction with Dr. Yojiro Yamanaka. Dr. Krawchuk assisted in the data analysis and other molecular biology experiments. Nobuko Yamanaka helped in the maintenance of the animal colonies. Microscopy training was provided by Cell Imaging and Analysis Network at McGill University.

LIST OF FIGURES

ABBREVIATIONS

2-Me	2-Mercaptoethanol
AVE	Anterior visceral endoderm
AU	Airy Units
BMP	Bone morphogenetic protein
Bra	Brachyury
CC	Cardiac crescent
Cer1	Cerberus-like
CO_2	Carbon Dioxide
d.p.c	Days post coitum
DA	Dorsal Aortae
DMEM	Dubelcco's Modified Eagle Medium
E	Embryonic day
EC	Endothelial cell(s)
EMT	Epithelial to mesenchymal transition
ESC	Embryonic stem cell
ETV2	ETS Translocation Variant 2
FCS	Fetal calf serum
FGF	Fibroblast growth factor
GFP	Green Fluorescence protein
HEPES	4-(2-hydroxyethyl)-1-piperazineethanesulfonic acid
iCre	Improved Cre recombinase
KDR	Kinase insert domain receptor
MEF2C	Myocyte-specific enhancer factor 2C
Mesp	Mesoderm Posterior
NE-AA	Non-essential amino acids
Nmyc	N-myc proto-oncogene protein
PS	Primitive streak
TGFβ	Transforming growth factor beta
Tie2	TEK tyrosine kinase, endothelial
VEGF	Vascular endotelial growth factor

VEGFR	Vascular endothelial growth factor receptor
Vg1	Vegetalising factor-1
Wnt	Wingless type
YS	Yolk sac

CHAPTER I

Introduction

1. *Overview of gastrulation*

After implantation, on embryonic day (E) 4.5, the mouse conceptus changes dramatically (Reviewed in [1]). At implantation the blastocyst consists of a vesicular structure with an inner cell mass located inside the trophectoderm. This structure then develops into an elongated one composed of the ectoplacental cone, which connects the embryo to the uterus, the extraembryonic ectoderm, the epiblast and the visceral endoderm. It is at this time that gastrulation starts.

Gastrulation, observed in all metazoans, is the process by which the three germ layers are formed: the endoderm, the mesoderm and the ectoderm [2]. Despite body shape and yolk content, amphibian and fish embryos are not very different from amniotes [3]. Generally, signaling during gastrulation is conserved among vertebrates [4]. In the mouse embryo, gastrulation commences when primitive streak develops at around E6.5 in the future posterior area of the embryo, and continues until E10.5 with the appearance of the tail-bud[5,6]. Adjacent cells coming from the epiblast move through the streak and form the mesoderm and endoderm. From the mesoderm, described in more detail subsequently, the endothelial cells, hematopietic, muscle, bone and kidney are derived [4]. The definitive endoderm is specified when cells from the epiblast ingress the anterior primitive streak

2. *Development of the pimitive streak*

The first step into gastrulation is the formation of the primitive streak, a structure that covers the posterior two thirds of the future midline [2]. Prior to its formation, a cluster of cells is detected in the posterior margin of the epiblast [7]. Afterwards, more cells accumulate from the posterior of the epiblast towards the future node. Identification of the first primitive streak forming cells has been done through the use of transplantation techniques in the whole chick embryo culture [2]. When a section of the posterior marginal zone of the blastodisc is transplanted in the anterior side of the embryo, an ectopic primitive streak-like structure develops[8]. Epiblast cells that formed the primitive streak internalize and generate the mesoderm and endoderm. The cells that remain in the epiblast become ectoderm [9].

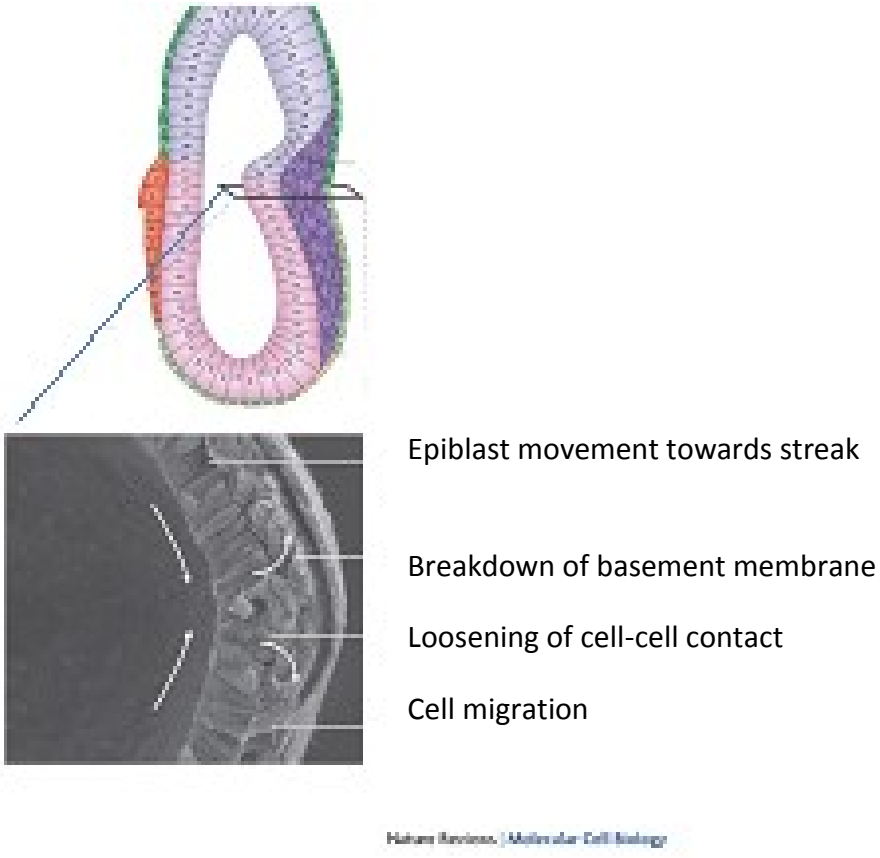

Fig. 1.1. Establishment of the mesoderm is achieved by ingression of epiblast cells through the primitive streak. During early gastrulation, polarized epiblast cells ingress into the primitive streak and undergo epithelial to mesenchymal transition. During epithelial to mesenchymal transition (EMT), cells lose their epithelial phenotype (basement membrane and polarization) and acquire mesenchymal characteristics, which include migratory capacity and invasiveness. After this transition, the cells exit the primitive streak and migrate away from it to contribute to different tissues of the developing embryo (image modified from [10]). The top image shows an embryo (E6.5). The pink denotes the epiblast and the purple the primitive streak. The bottom image shows a cross-section of the posterior section of an E6.5 gastrula embryo showing the ingression of epiblast cells into the primitive streak.

2.1. *Signaling involved in primitive streak formation*

Insight into the formation of the primitive streak has come from studies in chicks [4]. Mesoderm induction seems to be a prerequisite for streak formation. Manipulation studies that inhibit

mesoderm formation have resulted in the inhibition of the primitive streak, suggesting the role of mesodermal cells in its development[11]. For example, blocking fibroblast growth factor (FGF) signaling through FGF receptor inhibitors or depletion of FGF ligand results in the lack of mesoderm formation, and is associated with the absence of the primitive streak[12,13].

Induction of this structure has also been attributed in part to Wnt and Nodal signaling. It has been shown that Wnt8C expressed in the posterior marginal zone interacts with Vg1 to induce the primitive streak in chick embryos[14]. Wnt1 misexpressed in the area pellucida of the chick promotes formation of the primitive streak in response to Vg1[14]. Other posteriorly expressed molecules responsible for primitive streak induction are Activin and Chordin. In fact, implantation of COS cells (monkey kidney fibroblasts) overexpressing *Wnt8C, Vg1, Activin* and *Chordin* at the marginal zone of the blastodisc induces ectopic formation of the primitive streak, which copies the inducting activity seen in the posterior[15-18]. However, overexpression of Wnt8C alone is not enough to ectopically induce the structure; nevertheless, it enhances the inducing activity of overexpressed Vg1[14].

Nodal, a TGFβ superfamily molecule, acts downstream of Wnt and Vg1 and appears to play a key role in induction of the primitive streak[19]. *Nodal* mutants are known to fail to complete gastrulation and lack most of the mesoderm[20]. The phenotype can be rescued when *Nodal* expressing cells are transplanted in the region, suggesting that low amounts of the protein are enough to induce mesodermal formation[21]. In addition, the correct positioning of the primitive streak seems to be mediated in part by Nodal inhibitors secreted from the anterior visceral endoderm (AVE)[19]. Inhibition of Nodal blocks the formation of an ectopic primitive streak. Lefty1, another member of the TGFβ, and Cerberus-like (Cer1), are two antagonists of Nodal expressed and secreted by the AVE.. Cerberus-like$^{-/-}$; Lefty1$^{-/-}$ compound mutants develop ectopic primitive streaks. The rescue of the phenotype is achieved by removing one copy of the *Nodal* gene[22]. The results suggest that Cerberus-like and Lefty in the AVE restrict the primitive streak formation to the posterior side of the embryo by antagonizing Nodal signaling[22].

BMP-4 is another molecule important for the primitive streak formation. Prior to the formation of the primitive streak, BMP-4 is expressed at the streak; however, as the structure starts to form, its expression is downregulated; misexpression of BMP-4 in the posterior area results in the inhibition of the primitive streak formation and arrests the development of the Hensen's node

and axial structures[23]. BMP signaling is necessary for specification of derivates formed in the posterior part of the primitive streak. In mice, BMP-4 is required in mesoderm induction and mesoderm lineage differentiation[24].

2.2. Epithelial to mesenchymal transition (EMT) in the primitive streak

In order to form the mesoderm, epiblast cells must ingress through the primitive streak and undergo a process of EMT. EMT is a biological process that allows a polarized epithelial cell that contains a basement membrane to go through biochemical changes that include downregulation of cell-cell adhesion molecules and assume a mesenchymal cell phenotype, which is highly migratory, invasive and resistant to apoptosis[25]. As it was explained in the previous section, Wnt, Nodal and Vg1 signaling promote primitive streak formation and EMT. Additionally, Snail, Eomes and Mesp transcription factors regulate EMT.

Snail, discovered in *Drosophila* for its importance in the formation of the mesoderm, encodes for a transcription repressor of the zinc finger type[26]. Snail was found to directly repress *E-cadherin* expression, a gene encoding a cell-cell adhesion glycoprotein. In mouse embryos, Snail is present in undifferentiated mesoderm undergoing EMT, where E-cadherin is absent [27].

T-box transcription factor Eomesodermin (Eomes), initially identified in the Xenopus, has also been identified as an important factor of gem layer specification and patterning[28]. In Xenopus, Eomes has been described as sufficient and necessary for mesoderm formation[28]. In mouse, following implantation Eomes becomes restricted to the extraembryonic region and later induced in the posterior proximal epiblast prior to streak formation [29]. During gastrulation, *Eomes* is restricted to the primitive streak and the nascent mesoderm. In a study, the *Sox2:Cre* mouse strain was used to delete *Eomes* selectively in the epiblast. Upon Cre-mediated excision, *Eomes* was found to be not required for induction of mesodermal markers; however, nascent mesoderm failed to delaminate and migrate away from the primitive streak. Lack of mesodermal migration was linked to the lack of downregulation of *E-cadherin* and failure to undergo EMT[29].

Mesoderm posterior 1 (Mesp1*)*, a basic helix-loop-helix transcription factor, is expressed in mouse by cardiovascular progenitors from embryonic day (E) 6.5- 7.5[30]. A study done by Coleman et al. with differentiating embryonic stem cells (ESCs) identified that *Mesp1* promoted mesoderm and induced genetic changes associated with EMT, independently of Wnt signaling[31].

3. *Assembly of angioblasts into vascular structures, formation of vascular lumens and organization into networks: vasculogenesis*

Vasculogenesis is the process by which the first embryonic blood vessels are formed before the onset of blood circulation[32]. Endothelial cells are the forming unit of the blood vessels. In essence, vasculogenesis refers to the de-novo emergence of primordial endothelial cells and blood vessels that takes place in the mammalian extraembryonic region and within the embryo proper[33].

3.1. *Extraembryonic vasculogenesis*

In the mouse, a subset of mesodermal cells migrates away from the primitive streak to the extraembryonic region (reviewed in [34]). At E7.0-E7.5 angioblast precursors scatter throughout the mesoderm and in conjunction with erythrocyte precursors form the blood island, a belt-like structure that encircles the yolk sac[35]. Within the blood island, nestled by the outer visceral endoderm and an inner mesothelial cell layer, endothelial cells and primitive erythrocytes develop. Endothelial cells within the blood island assemble at their future location, where they give rise to developing vessels[36]. As an overall structure, and due to the endothelial cells, the blood island undergoes extensive remodeling, which results in the formation of the primary plexus, a network of endothelium within which blood cells circulate. Extra-embyronic vasculogenesis also occurs within the allantois, a structure located at the posterior side of the embryo that contributes to the formation of the umbilical vessels[37].

3.2. Embryonic vasculogenesis

Within the embryo proper, the heart and the dorsal aortae are the first vascular structures to develop. At E7.5, de-novo angioblasts arise throughout the mesoderm and aggregate close to the midline, forming loosely organized vascular cords[38]. Endothelial precursors within vascular cords form further contact with others, remodeling them into tubular structures. Further remodeling of the tubular structures occurs and two longitudinal trunk axial unbranched vessels lying ventral to the notochord are formed, thus creating the dorsal aortae[39]. Later in development, at around E9.5, the angioblasts fuse and form the descending aorta, the largest vessel in the mammalian trunk[40].

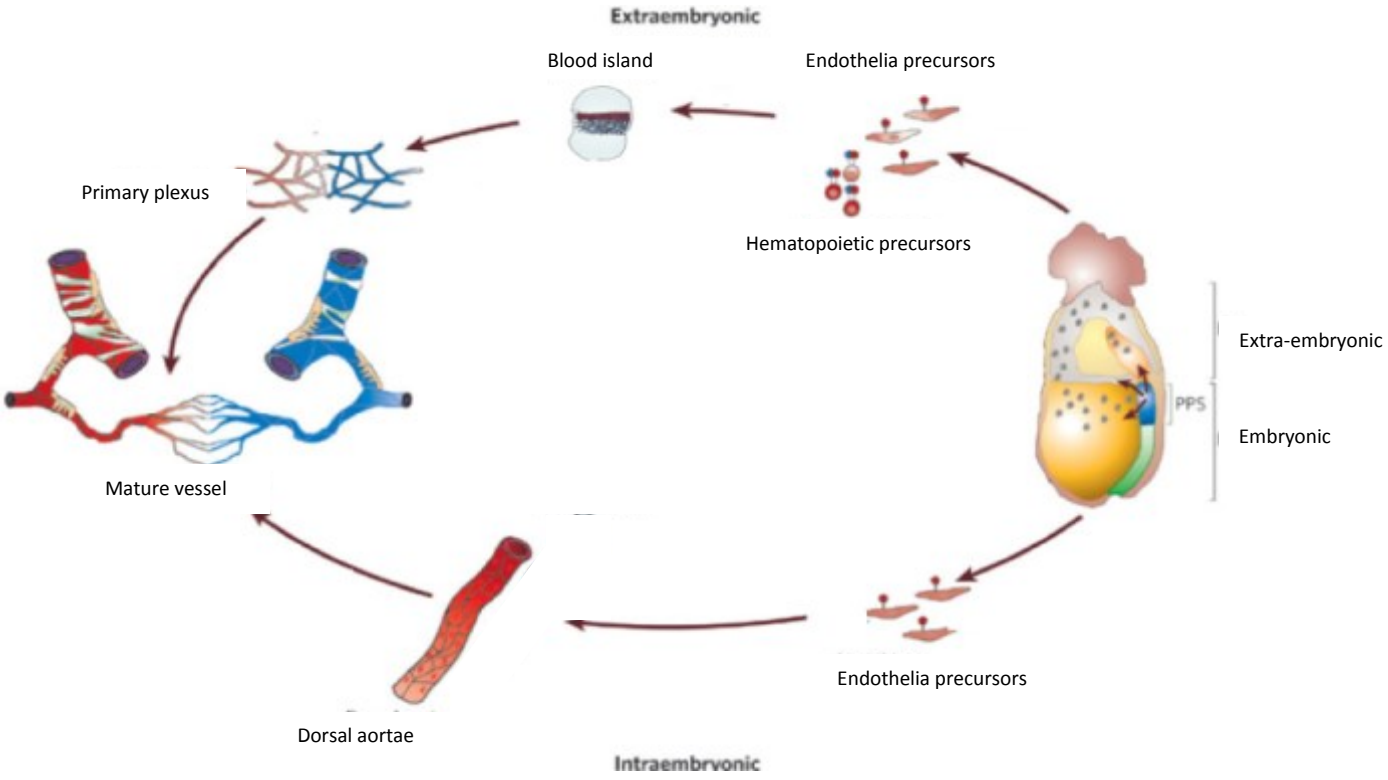

Fig. 1.2. Extra-emrbyonic and embryonic vasculogenesis. Mesodermal cells migrate from the primitive streak and establish the blood island in the extra-embryonic region. Blood islands coalesce and form the primary plexus that further remodels into mature vessels. Within the embryo, endothelial precursors form two unbranched tubular structures lateral to the midline, the primitive streak, which later in development becomes the descending aorta. Image modified from[41].

3.3.Signals controlling vasculogenesis

3.3.1. VEGF

Vasculogenesis seems to be largely dependent on VEGF signaling. Vascular endothelial growth factor-A (Vegf-A) was the first growth factor shown to have direct influence on the endothelial lineage specifically[42]. The VEGF family is a group of homodimeric glycoproteins whose activity is essential for the formation and remodeling of the vascular system. The family comprises 4 VEGF ligands (A-D) and a related growth factor, placenta growth factor (Plgf). The ligands bind to 3 structurally related receptors: VEGF-receptor-1, 2 and 3 (VEGFR1-3) and other co-receptors like neuropilins. These receptors induce cellular processes including cell migration,

survival and proliferation[43]. VEGFR-1 can be found expressed in endothelial cells, monocytes and macrophages, while VEGFR-2 is found in endothelial cells and VEGFR-3 restricted to lymphatic endothelial cells[43].

Vegfa$^{+/-}$ embryos result in embryonic lethality between E11 and E12. These embryos exhibit defective vascularization and reduced number of red blood cells in the yolk sac. *Vegfr-1/Flt-1* null mice die in uterus between E8.5 and E9.5 due to incremented numbers of mesodermal cells that become angioblasts, leading to disorganized highly dense blood vessels [44]. Lack of *Flt-1,* however, does not block EC differentiation. Signaling of VEGF, through *Vegfr-2*/*Flk-1*/*KDR*, is indispensable for EC generation and vessel development[45,46]. Deficiency in *Flk-1* results in embryonic death because the endothelial and hematopoietic lineages do not develop[34]. A chimeric aggregation study using wild type embryos showed that *Flk-1* null cells were not able to form any vessel or hematopoiesis[45]. These studies prove the necessity of this receptor in EC specification.

3.3.2. ETV-2/ER-71

ETS variant 2 (*Etv-2*), also known as *ER-71*, forms part of a group of transcription factors known to contain a short stretch of 85 amino acids called E-26-specific DNA-binding domain (ETS)[47,48]. Among the ETS factors, *Etv-2*, initially identified in the testes [49,50], has been implicated in the differentiation of mesodermal cells towards the EC fate[33]. *Etv-2* is initially detected within the posterior mesoderm[51]. Later its expression gets restricted to the extraembryonic mesoderm, lateral plate mesoderm, and cardiac crescent in embryos (between E7.0 and E7.75)[52] before it finally gets confined to major blood vessels[53]. These studies also identified that *ETV-2* expressing cells were also expressed *Flk-1*, consistent with its importance in vascular development[33].

In zebrafish embryos, morpholino knockdowns or mutation within the *etsrp (Etv-2)* gene results in loss of expression of endothelial cell markers, including *VE-cadherin* and *Flk-1* [51,54]. In mice, the absence of *Etv-2* results in FLK-1+ cells downregulating endothelial genes[53]. Mice deficient in *Etv-2* die between E9.0 and E10.5 and lack endothelial cells, resulting in the absence of the primitive streak, yolk sac vasculature and endocardium, although the mesoderm is present[52]. Overexpression of ETV-2 leads to ectopic expression of endothelial markers in different animal models[51,53,54].

The time window for the expression of *Etv-2* is critical for proper vessel development[33]. *Etv-2* is rapidly downregulated once EC have been specified[53]. Constitutive expression of *Etv-2* under the promoter of *Tie2* (a vascular endothelium marker) results in impaired remodeling of the extraembryonic vasculature with dilated blood vessels, leading to lethality[55].

4. Cardiogenesis

The heart, in conjunction with the vasculature, is the first organ to develop in the embryo. A series of complex morphogenetic processes allow the heart to be formed by the mesoderm.

During gastrulation the mesoderm, destined to become cardiac progenitors derived from the epiblast, ingresses into the cranial and middle sides of the primitive streak[56]. Once the mesoderm exits the primitive streak at E6.5-E7.5, the cells migrate into the antero-lateral area of the embryo[1,57,58].

Just before somite formation, cardiac progenitors organize as part of the inner splanchnic and the outer somatic lateral plate mesoderm[58]. Both layers fold ventrally and fuse at the midline, forming a horseshoe shape called the cardiac crescent[59,60]. The heart tube forms when the crescent undergoes conversion and fusion at the midline[61]. In all vertebrates, the heart tube undergoes a process of rightwards looping, while more cardiac progenitors originated from the pharynx join the forming structure[62]. This is particularly true in chicks where the heart can be seen going from a linear structure that gradually loops[63]. In mice, however, because of the short distance between the head-fold and the forming foregut, the heart forms two bulges at the midline, then fuses to create one bulge (the linear heart tube seen in chicks) that immediately starts to loop[58,60]. At this point the heart is composed of an inner endothelial layer, the endocardium, and the outer myocardial layer. The heart then remodels and develops chambers via formation of the atrio-ventricular canal, endocardial cushions (act as precursors of the 4 major heart valves: the aortic, pulmonary tricuspid and mitral valves), trabeculae (lining of the ventricle by myocardial protrusions), septation of the atria and ventricles, and finally remodeling of the outflow tract (allows the formation of the aortic and pulmonary arteries)[62].

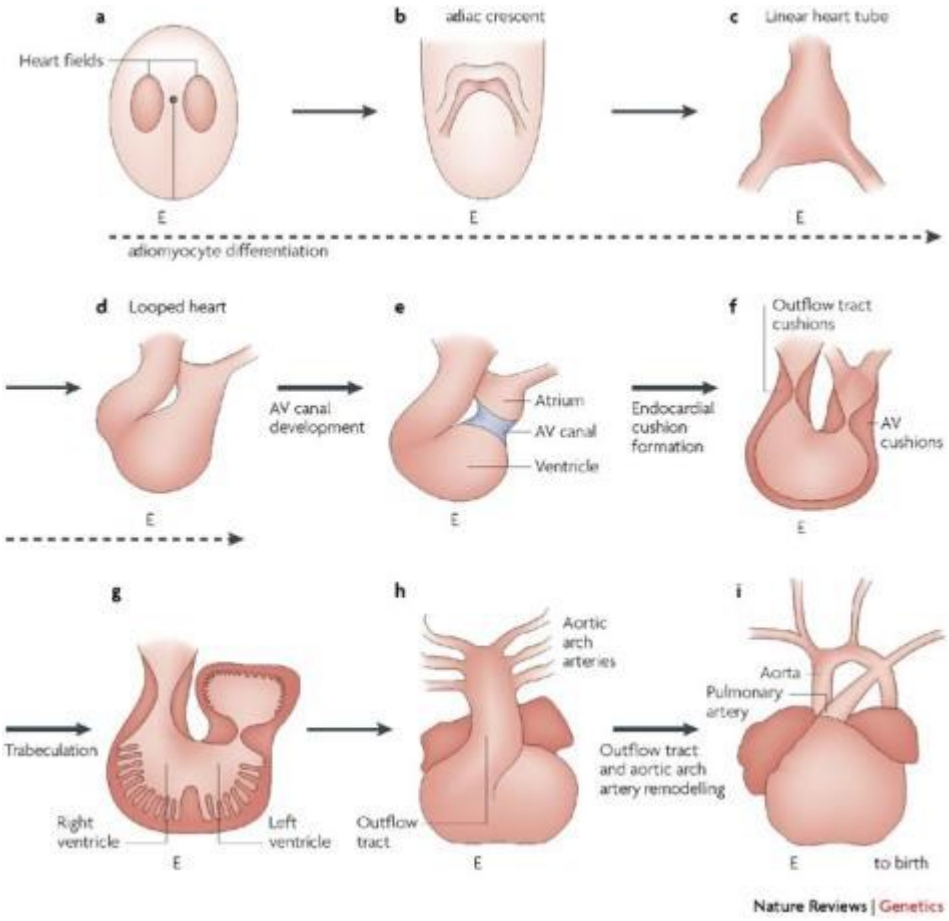

Fig. 1.3. Main stages of cardiac development. From a-i: Mesodermal heart progenitors exit the primitive streak and localize to the anterior-lateral side of the embryo at 7.0. The progenitors fuse at the midline, forming the cardiac crescent. The heart tube is then formed and loops. The atrioventricular canals develop and the endocardium cushions are formed, followed by myocardium trabeculation. Finally the outflow tract and the aortic arch artery remodel to give rise to the mature heart. Image taken from [62]

4.1. Signals regulating cardiogenesis

Genes encoding factors of the NK homeodomain, Gata and T-box have been found to be important in the specification and patterning of the heart.

4.1.1. NK Homeodomain proteins

Tinman, the first cardiac related NK homeodomain gene was identified in *Drosophila*.-*Tinman* is required for the establishment of the dorsal vessel which is the equivalent of the heart tube in

vertebrates [64]. In *Drosophila*, expression of this gene is found during gastrulation in most of the mesoderm. Its expression then gets restricted to the cardiogenic, visceral and dorsal body wall muscle mesoderm before it is further restricted to the precursor cells of the dorsal vessel. Lack of *tinman* blocks heart formation.

Vertebrates contain various member of this subgroup of homeobox genes called *Nkx2.3-Nkx2.10*. In mouse, the *tinman* homologs involved in cardiogenesis include *Nkx2.5* and *Nkx2.3*, which appear in the embryo at E7.5, E8.0 and E9.5, respectively[65]. *Nkx2.5* is expressed in the lateral plate mesoderm within the cardiac field and continues to be expressed in the heart throughout development[66]. Different from *tinman* mutant phenotypes, lack of *Nkx2.5* in mouse embryo leads to cardiogenic arrest prior to cardiac looping[67]. Although commitment of cardiomyocyte precursors is not abolished, several myocardial genes are downregulated in the heart of *Nkx2.5* deficient embryos, including *myosin light chain 2*, *MEF2C, Hand1, Nmyc*, and others [67-70].

The milder phonotype raises the question about redundancy between *Nkx2.5* and other members of the *Nkx2* group[61]. Double mutant mouse embryos *Nkx2.5;Nkx2.6* display a slightly more severe phonotype than *Nkx2.5*$^{-/-}$embryos[71]. These results suggest the existence of limited redundancy between members of the NKX2 genes in heart development. Increasing evidence, however, seems to point protein interactions between *Nkx2.5* and other cardiogenic transcription factors, like Gata factors, as important factors during cardiogenesis[61].

4.1.2. *Gata factors*

Gata proteins are transactivation factors that regulated different processes in the developing embryo[72]. Gata4, 5 and 6 are important for cargiogenesis[73-75]. *Gata4, 5* and *6* are expressed in the precardiac mesoderm at the same time and in the same place, as *Nkx2.5*[76,77]. Knockout of *Gata4*, in mouse and *Gata5* in zebrafish show early heart defects and decrease of *Nkx2.5* expression with vascular defects[73,78]. Moreover, knockdown of *Gata 4, 5* and *6* simultaneously results in the failure of the heart tube assembly and failure of the mesoderm to fuse at the midline, resulting in cardia bifida [79].

4.1.3. T-box factors

Mutations in Tbox genes, *TBX1* and *TBX5* in humans are associated with cardiac defects: DiGeorge and Holt-Oram syndromes, respectively[80,81]. *Tbx5* is expressed in the bilateral cardiac

primordia, where *Nkx2.5* and *Gata* genes are also found[82]. Moreover, *Tbx5*$^{-/-}$mouse embryos display hypoplasia, severely deformed hearts and reduction of *myosin light chain 2*, *Nkx2.5* and *Gata4* expression.

4.2. Development of the endocardium

The endocardium forms the inner walls of the heart and is composed of endothelial cells. Vasculogenesis and endothelial specification, explained previously, are necessary for the endocardium formation. In the embryo, angioblasts are specified within the cardiac crescent and become endothelial cells in a similar de-novo vasculogenic process, as seen in the extraembryonic region[58]. The unique location of the endocardium has led investigators to think that the endorcardium progenitors are more than a subset of endothelial cells; in fact, it is thought that the endothelial cells are of a different molecular profile[83]. For example, *Tie* and *Tie2* are two genes involved in vasculature during late organogenesis. *Tie*$^{-/-}$;*Tie2*$^{-/-}$ embryos display normal extracardiac vasculogenesis but also display deficient endocardium; in these embryos endothelial cells contribute to all the other vascular structures. In support of this notion, *cloche* mutants also show lack of endocardium and normal development of the dorsal aortae and cardinal veins[84]. However, in contrast with these results, to date no gene or factor has been identified as dispensable for endocardium development and essential for vessel specification in other areas of the embryo[83].

5. Summary of objectives

The objectives of my research are to characterize the *in-vivo* behavior of *Flk-1* positive cells and to create a fate map of these cells during cardiac and vascular formation. To achieve this goal the *Flk-1*-GFP mouse reporter line will be used, which is the GFP knock-in mouse line into the endogenous *Flk-1*locus. Live-imaging will be achieved with the use of confocal microscopy. We hypothesize *Flk-1*-GFP+ cells will have different origins within the mouse gastrula and will contribute to multiple lineages.

CHAPTER II

Protocol for *ex-utero* live-imaging of mouse gastrula embryos

1. Introduction

Gastrulation is marked by the formation of the primitive streak, a transient structure that develops at the posterior end of the embryo[1]. Epiblast cells ingress through this structure, where a process of epithelia to mesenchymal transition commences and culminates with the establishment of the three germ layers: the ectoderm, the mesoderm and the endoderm (Reviewed in [10]). During this highly dynamic process, cells undergo proliferation, apoptosis, migration and differentiation; likewise, their fates are determined and roles are assigned for future organ development[85].

Although major events of gastrulation are evolutionary conserved in vertebrates, mammalian embryos also show unique developmental processes. Studying mammalian gastrulation is challenging[86]. Due to its uterine implantation and small size mammalian, embryos are situated in an inaccessible place to study them in their intrinsic environment[87]. Thankfully, dissection and culture techniques have been developed to extract embryos from the uterus without compromising the integrity of the organism. Mouse embryos, commonly used in developmental studies, propose a further challenge. Immediately after post-implantation, the mouse conceptus (~5 d.p.c.) transforms from a circular vesicular blastocyst into a cup-shaped structure[1]. The newly formed shape prevails during gastrulation and organogenesis, thus impeding upright positioning of the embryo during experiments.

With the development of fluorescence microscopy in the 1980s and mouse reporter lines in the 1990s, defined cell populations are now traceable, disclosing important information about specific events during gastrulation[86]. Yet, as a result of being cup-shaped, mouse embryos pose a real challenge to live microscopy because they are not able to hold themselves in a specific orientation without moving. To successfully observe mouse gastrulation processes in the distal and lateral regions under the microscope, a mounting technique was developed in our laboratory in which the embryo is held statically without damage or restraining its growth. A summary of the technique is presented in Figure 2.1.

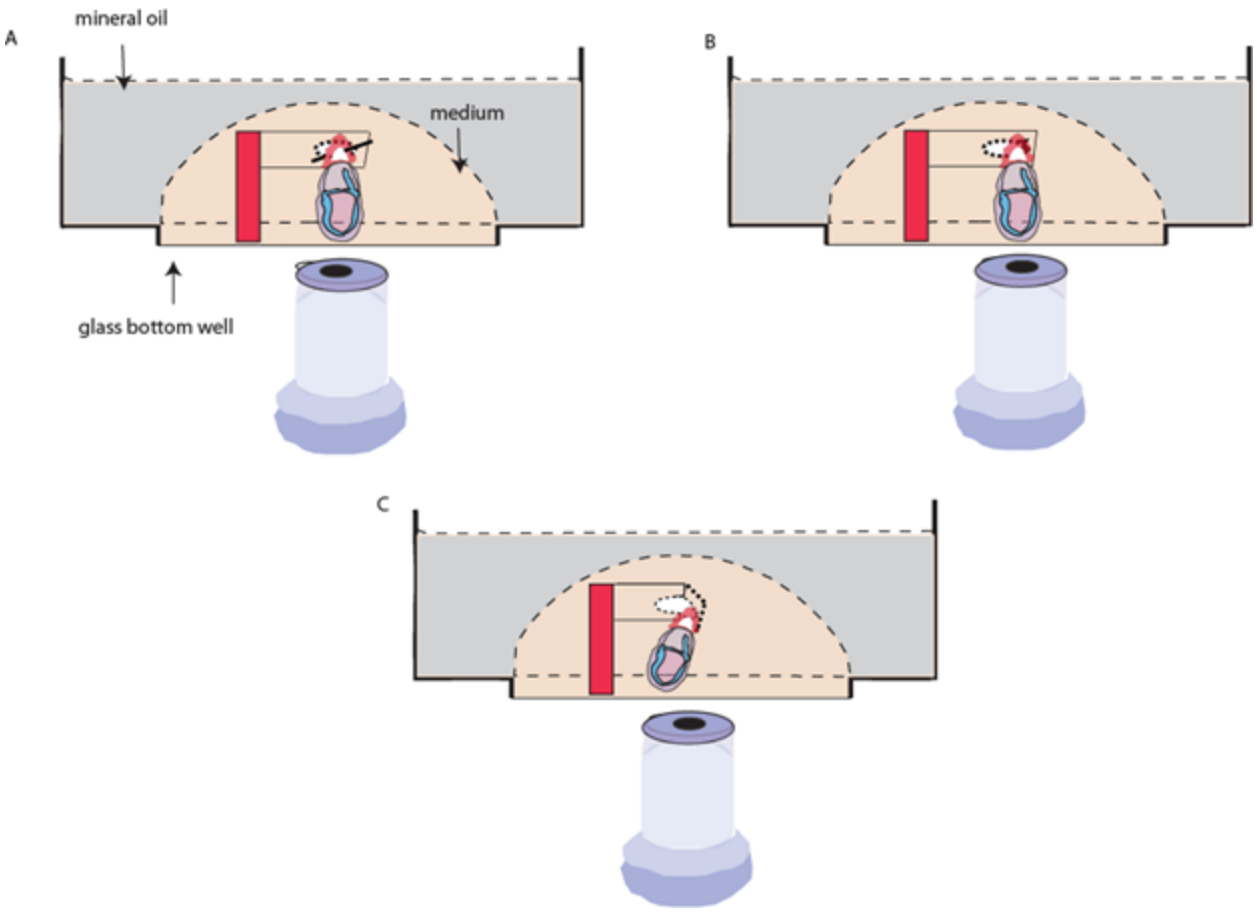

Fig. 2.1. **Schematic representation of the mounting of embryos at E7.5**. A) To observe the distal area, a small piece of eyelash (~1mm) is cut and used to perforate the ectoplacental cone. The embryo is hanged from the small silicone stage containing a protruding clear plastic that contains a small circular perforation. B) A variation of the technique explained above. Here, however, a side of the circular perforation is slightly burnt to create a small cavity in which the ectoplacental cone is held. C) Technique to image the anterior, posterior and lateral sides of the embryo. To visualize these areas, the clear plastic protruding from the silicon stage is bent downwards 45°. A small cavity is produced by burning the side of the bent plastic, from which the ectoplacental cone will hang. In each technique, the embryo is imaged in a glass bottom dish containing medium which is covered by a layer of mineral oil to avoid evaporation.

2. *Materials*

2.1. Reagents

Mice (wild-type or reporter/mutant strains)

Gastrula or early organogenesis mouse embryos

Dubelco's Phosphate-buffered saline (D-PBS) without calcium and magnesium (Wisent)

DMEM - Dulbecco's Modified Eagle Medium without phenol red (Wisent)

DMEM - Dulbecco's Modified Eagle Medium with phenol red (Wisent)

Fetal calf serum (FCS) (Gibco)

Immediately centrifuged rat serum (heat inactivated)

GlutaMAX- L-glutamine replacement (Invitrogen)

2-ME (Sigma) (Invitrogen)

Nonessential amino acids (NE AA) (Invitrogen)

Mineral oil

4-(2-hydroxyethyl)-1-piperazineethanesulfonic acid (HEPES) (pH 7.5)

5% CO_2 (in mixed air)

Ethanol (70% v/v)

2.2.Equipment

Dissection tools:

F.S.T. Fine tip forceps Dumont #5 (biologie tip)

F.S.T. Cohan-Vannas scissors

F.S.T. Fine Scissors - Martensitic Stainless Steel,

30 Gauge needles (insulin needles)

Secure-Seal™ hybridization chamber gasket, eight chambers, 9 mm diameter, 0.8 mm deep

Dissection microscope

Confocal microscope or point scanner

Bunsen burner

Mattek glass bottom microwell dish 35mm petri dish, 10mm microwell No. 1.5 coverglass.

200µl pipette tips.

50mm petri dish

2.3.Reagents setup

Mice and embryo generation. To obtain the desired embryonic stage, the mouse mating is timed. Based on the day/night cycle, female mice ovulate closer to midnight; this is considered the time at which mice mate, so the set up should be performed later in the afternoon. After successful copulation, male mice leave a plug in the vagina of the female mice. The discovery of the plug, the morning after mating, is considered embryonic stage (E) 0.5 (at 12:00PM). Female pregnant mice are sacrificed by cervical dislocation, and gastrula or early organogenesis embryos (6.5-9.0 d.p.c) are dissected from the uterus. Embryos are delicate and therefore handling should be performed with great care. Embryonic litter size varies depending on the strain of the animal.

Uterine dissection medium. Dissection of the maternal uterine horns to extract the deciduum should be performed in D-PBS (with calcium and magnesium); meanwhile, extraction of the embryo from the deciduum should be performed in embryonic dissecting media (explained below).

Dissection medium. In a total volume of 500mL DMEM with phenol red, make a 10mM solution of HEPES with 5%FBS. The solution can be stored at 4ºC for at least 6 months. Usually, the amount of dissection medium used per dissection does not surpass the 35ml mark.

Live-imaging culture medium. Combine a total volume of 400µl composed of 40% DMEM without phenol red, 10% FCS, and 50% immediately centrifuged rat serum (after heart perfusion and subsequently heat inactivated), 2mM GlutaMAX, 0.1mM 2-ME, and 1mM sodium pyruvate and 0.1mM NE AA. Pre-warm the solution to room temperature prior to dissection of the embryo. It is recommended to use freshly prepared culture medium every time an experiment is done; however a stock solution of 80% DMEM without phenol red, 20% FCS, 4mM GlutaMAX, 0.2mM 2-ME, 2mM sodium pyruvate and 0.2mM NE AA can be prepared and store at 4ºC for at least 4 months. The solution should be prepared under sterile conditions. If necessary, filter the rat serum to obtain superior purity.

3. Equipment set up

Microscope. Leica DMI6000B with WaveFX spinning disk confocal system equipped with 4 lasers, 440nm (15mW), 491nm (25mW), 561nm (50mW), 638nm (30mW) and Nikon Eclipse Ti Swept Field confocal equipped with 4 lasers 405nm, 488nm, 561nm and 640nm have been used for our purposes; however, other microscopes with comparable settings can be employed. Similarly, different objectives can be employed. Here, we used objectives: 10X NA 0.4 dry, 20X NA 0.7 dry when using Leica and Fluor 10X NA 0.50 dry and Plan APO 20X NA 0.75 dry in the Nikon system.

The microscope needs to be assembled with an external incubation chamber as well as a stage incubation chamber to avoid temperature fluctuations. The temperature inside the external incubation chamber, as well as the stage incubation chamber, should be maintained at 37°C for the entire duration of the experiment. The stage incubator must also have a gas exchange line though which 5%CO_2 can be administered. The system should be warmed up with these settings at least 1 hour before the sample is placed inside.

The following image settings were used to image embryos in our experiment using *Flk-1*-GFP reporter line. With both equipment, an interval of 10-15μm was used for a 24 hour period with a Z-range (total depth of imaging) of ~200 μm. The interval acquisition time was set for 10 minutes. The camera scan speed was set up for 10MHz (although lower frequency was employed with the same reporter line in other experiments). In a spinning disk confocal the pinhole is fixed to 1 airy unit (AU). The Swept-field technology, however, is equipped with different pinhole sizes and slits which allows the increase of AU. To be able to detect a weaker signal, we chose to use a 50μm wide slit.

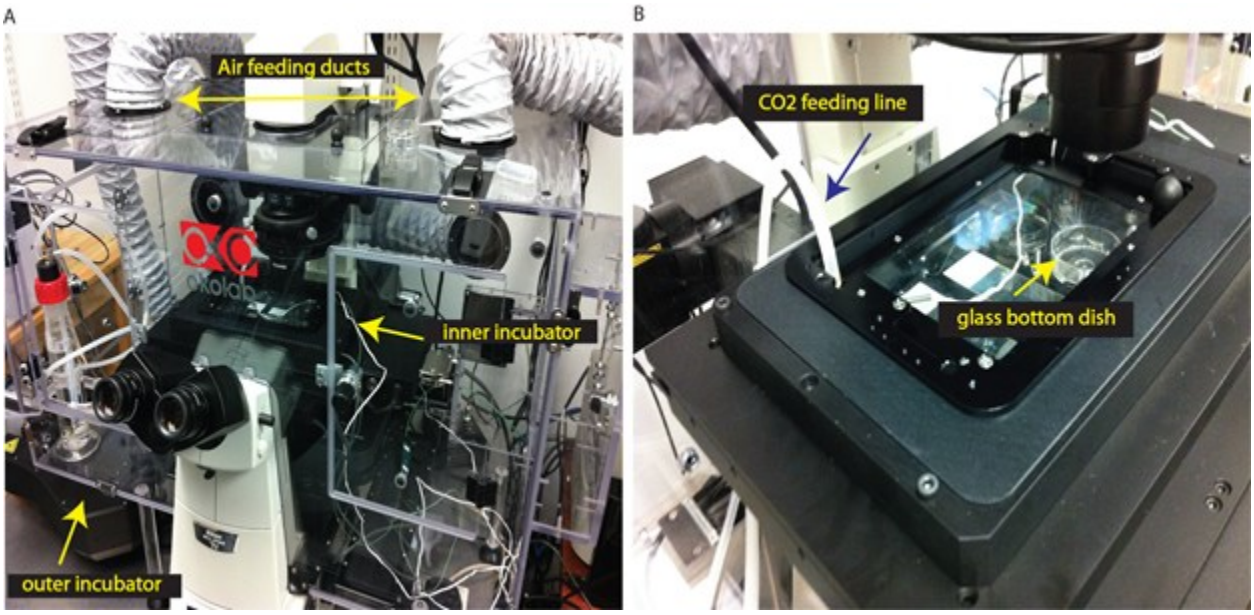

Fig. 2.2. Incubation system attached to a confocal swept field Nikon microscope. A) Nikon microscope equipped with and outer incubator with air feeding ducts to introduce warm air to keep a constant 37°C temperature. The outer chamber should be as sealed and apertures minimized as permissible. B) Inside the outer incubator and inner incubator with its own temperature and gas exchange controller to maintain a constant 37°C and 5% CO_2. The inner incubator should also be as airtight as possible, to avoid heat escape.

Embryo transfer-pipette. To transfer embryos from one place to another, cut the tip of a pipette tip (we usually use a 200µL tip). Three or four mm should be sufficient to allow the entrance of an E7.5 embryo. For later stages increase the cut size, suitable for the size of the embryo.

4. Embryo set up

1. Sacrifice pregnant dam at gastrulation or early organogenesis (E6.5-E8.5). Euthanasia methods should follow the rules of the institution and/or the local authorities. The technique should be done as effective as possible to reduce suffering to the animals. We perform cervical dislocation; however, other methods, like asphyxiation by CO_2, are also possible.
2. Disinfect the lower abdominal area with ethanol (70% v/v)

3. With fine scissors, make a small fissure on the skin of the mouse. Using your fingers, pull each side of the skin in opposite direction to open the area and expose the muscle wall covering the peritoneum. Likewise, instead of pulling the skin to open it, a transverse incision on the lower abdomen can be done with a pair of scissors.
4. With forceps, pull the muscle layer away from the organs and with the scissors open transversally the muscle layer, exposing the organs.
5. Push the intestines towards the chest of the animal, away from the uterine area, to uncover the decidua-filled uterine horns.
6. To avoid damaging embryos, use forceps to hold the uterus in between two decidua. Never hold the uterine horn through a deciduum. With scissors remove the vascular tissue that surrounds uterine horns, cut the site of fusion between the uterine horns and the ovaries, and cut the connection between the uterine horns and the uterus body. Remove as much uterine tissue as possible to facilitate visualization during dissection.
7. Place the uterine horns in a 50mm petri dish filled with D-PBS.
8. With the aid from two pairs of forceps, open the uterus from the vascular side of the uterus to avoid damage to the embryo. The uterine horns have a vascular and a muscular side. The embryos, sitting inside the deciduum, are positioned away from the vascular side of the uterine horn. To avoid unintended damage when extracting the decidua, open the uterine horns from the vascular side.
9. Using forceps transfer the decidua to a clean 50mm petri dish filled with dissecting media. Hold the deciduum by the thicker area, away from the embryo.
10. With a pair of forceps hold down the embryonic side of the deciduum without touching the embryo. On the opposite side of the deciduum, make an incision perpendicular to the embryo with the other pair of forceps; this will open the deciduum on the opposite side of the embryo and diminish the possibility of damage.
11. While still holding the deciduum on the embryonic side, slide the forceps through the incision previously made to cut the deciduum along the boundary between the embryo and the maternal tissue. Be careful not to pierce the embryo. If not done carefully, there is a risk of perforating the yolk sac or the embryo proper, making the specimen unviable for this experiment.
12. While still holding the deciduum on the embryonic side, remove the embryo with the other pair of forceps from the deciduum.

13. Once the embryo has been exposed, with one needle (30-gauge) gently push down the Reichert's membrane without damaging the embryo. With another needle of the same gauge, and while still pushing down, rupture the membrane and remove it to uncover the embryo. Be careful not to pierce the embryo. If not done carefully, there is a risk of perforating the yolk sac or the embryo proper, making the embryo unviable for this experiment. Make sure to keep the ectoplacental cone.
14. If using reporter lines, use a fluorescence microscope to identify the fluorescent embryos.

I. Embryo mounting stage preparation: imaging the distal region of the embryo

To observe different sides of the embryo under the microscope, we have created variations of the same technique.

Be sure to pre-warm the embryo imaging media, at least 30 minutes prior to dissection.

Eyelash mounting

1. Cut the Secure-Seal™ hybridization chamber gasket into a fragment that contains at least 1-2mm^2 of silicone with the circular aperture intact. Leave ~0.5mm of clear plastic on the opposite edge of the silicon (Fig. 2.3. A)
2. Separate the perfusion chamber from the adhesive cover and adhere it on a glass bottom dish, with the silicone side closer to the edge of union between the plastic and the glass (Fig. 2.3. B, C and E)
3. Fill the area of the glass microwell with live-imaging culture medium. Make sure to cover the entire silicon setting with 100-125µl of media. Due to capillary action, a droplet will be created.

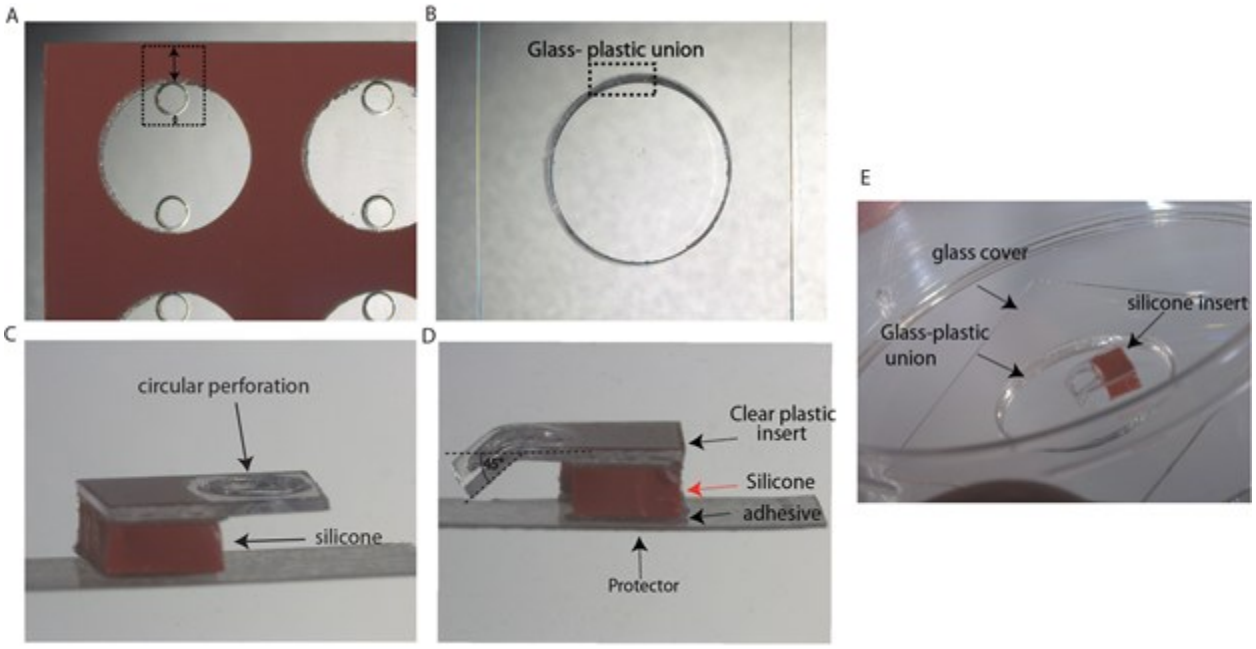

Fig. 2.3. Silicone stage set up. A) The chamber gasket is cut leaving the perfusion intact and including 1-2 mm of the silicone. B) Glass bottom dishes contain a border between the plastic of the petri dish and the cover-slide, which creates a second, smaller, microwell. C) Chamber gasket cut into the silicone stage intended for the visualization of the distal area of the embryo. D) Silicone stage made to visualize anterior, posterior and lateral areas of the embryo. The plastic is bent using the middle of the perforation as the axis guide. E) Silicon stage set up in the 35mm glass bottom dish. The silicon side of the stage should be placed close to the glass-plastic union. When imaging the more proximal areas of the embryo, it is important to melt the area of the plastic prior to the administration of the media to the well.

4. Take a human eyelash, preferably, from a person that has thick eyelashes.
5. Disinfect the eyelash with ethanol (70%v/v) and trim it to a length of 0.5-0.8mm (Fig. 2.4. A).The rest of the eyelash can be stored for indefinite time. At the moment of usage always disinfect it with ethanol (70%v/v)
6. With a pipette, transfer the embryo from the petri dish where the dissection was done to the glass bottom dish filled with live-imaging culture medium (Fig. 2.4. B**).** Try to add the least amount of dissecting media to the glass bottom dish containing live-imaging culture media.
7. Take the eyelash fragment and use it to puncture through the ectoplacental cone, in a horizontal manner (Fig. 2.4. C). Do not place the middle of the eyelash in the center of the ectoplacental cone; instead, leave most of it outside so it can be a better anchor point. (See

size ratio denoted by * and ** in Fig. 2.4. D). Be Careful not to damage the embryonic tissue closer to the ectoplacental cone.

8. Using forceps, needles (30-gauge) or a combination of both, insert the embryo putting the longer side of the eyelash on top of the clear plastic. It is important to take into consideration that the embryo needs to hang, but at the same time its distal tip should be loosely touching the glass of the dish. This will avoid unwanted movement during growth, leading to an out-of-focus image. If the embryo is not touching the glass, repeat step 7 (in this section). Take out the eyelash from the ectoplacental cone and re-puncture it in a higher area. If, on the contrary, the embryo seems not to fit the height of the mounting stage, re-puncture the eyelash somewhere lower in the ectoplacental cone.
9. To prevent evaporation of the media, fill the glass bottom dish with mineral oil. Make sure to cover the entire droplet of media.

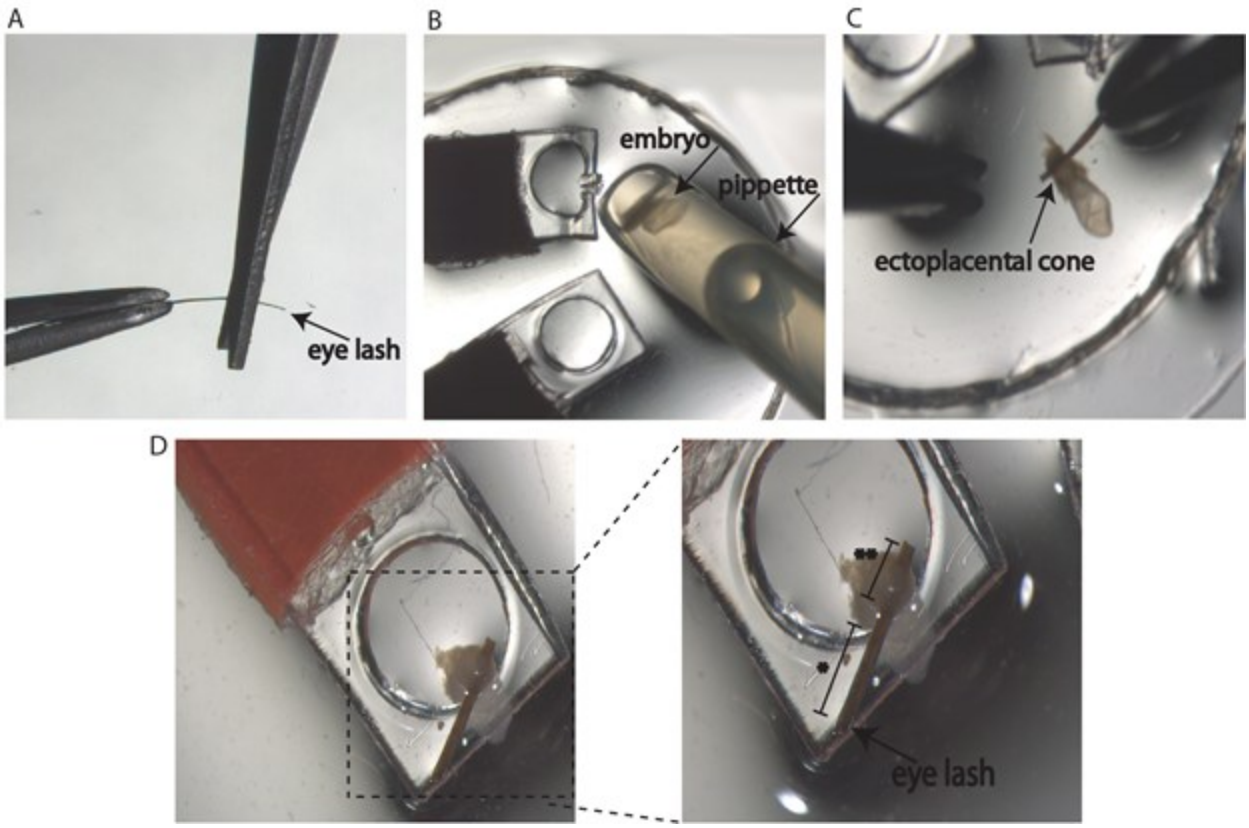

Fig. 2.4. Summary eyelash mounting process, step-by-step. A) The eye lash is trimmed to a size of ~1.0mm. Some eyelashes are thicker than others, and we have noticed that thicker ones puncture better. B) The embryo is transferred from the dish containing dissecting

medium to the glass bottom dish whose microwell has been filled with live-imaging culture medium. C) Using the trimmed eyelash, the ectoplacental cone is punctured horizontally. D) The longer part of the eyelash protruding from the embryo serves as anchorage (*) and it is placed on top of the clear plastic. This setting leaves the embryo hanging, and relatively free to move, yet strongly held in a certain position (**).

Rough-surfaced cavity mounting

When there is presence of brusque movements the eyelash method may not be strong enough to withhold the motion, and the embryo may dismount. The variation of the previous technique allows a wider range of motions, including short distance walks from one place to another, therefore decreasing the necessity of preparing the embryo in the same area as the location of the microscope.

1. Cut the Secure-Seal™ hybridization chamber gasket into a fragment that contains at least 1-2mm^2 of silicone with the circular aperture intact. Leave ~0.5mm of clear plastic on the opposite edge of the silicon (Fig. 2.3.A)
2. Separate the perfusion chamber from the adhesive cover and adhere it to the glass bottom dish, with the silicone side closer to the union between the plastic and the glass.
3. Using a Bunsen burner, heat the tip of a needle (30-gauge) and quickly melt the inner side of the plastic hole most distant to the silicone. This creates a small but rough cavity. To assure a successful melting of the plastic, the needle needs to turn orange under the flame. This will indicate the temperature within the needle is hot enough to melt the plastic. The size of the melt cavity should vary depending on the size of the ectoplacental cone of the embryo, the bigger the ectoplacental cone, the larger the cavity can be.
4. Fill the area of the glass microwell with live-imaging culture medium. Make sure to cover the entire silicon setting with 100-125µl of media. Due to capillary action, a droplet will be formed.
5. With a pipette, transfer the embryo from the petri dish where the dissection was done to the glass bottom dish filled with live-imaging culture medium. Try to add the least amount of dissecting media to the glass bottom dish containing live-imaging culture media.
6. Using forceps, needles (30-gauge) or a combination of both, insert the embryo, putting the placental cone through the plastic aperture and suspended. It is important to take into consideration that the embryo needs to hang, but at the same time its distal tip should be

loosely touching the glass of the dish. This will avoid unwanted movement during growth, leading to an out-of-focus image. If the embryo is not touching the glass, use a higher section of the ectoplacental cone and use this part to place it through the aperture. If on the contrary, the embryo seems not to fit the height of the mounting stage, place a lower area of the ectoplacental cone.

7. To prevent evaporation of the medium, fill the glass bottom dish with mineral oil. Make sure to cover the entire liquid of the medium.

II. Embryo mounting stage preparation: imaging the distal region of the embryo

Rough-surfaced bent cavity mounting

1. Cut the Secure-Seal™ hybridization chamber gasket into a fragment that contains at least 1-2mm^2 of silicone with the circular aperture intact. Leave ~0.5mm of clear plastic on the opposite edge of the silicon (Fig. 2.3. A)
2. Bend the protruding plastic that comes out of the silicone 45 degrees downwards (Fig. 2.3. D), using the middle of the diameter as the bending axis (Fig. 2.5. A). Depending on the size of the embryo and area, the degrees of curvature vary. It is important to take into consideration that the embryo needs to be held from the top and at the same time barely touch the bottom of the glass.
3. Separate the perfusion chamber from the adhesive cover and adhere it to the glass bottom of the dish, placing it with the silicone side closer to the union between the plastic and the glass.
4. Using a Bunsen burner, burn the tip of a needle (30-gauge) and quickly melt the side of the plastic hole most distant from the silicone. This creates a small but rough cavity. The size of the melt cavity should vary depending on the size of the ectoplacental cone of the embryo, the bigger the ectoplacental cone, the larger the cavity should be. However, the most important aspect of this step is the creation of the rough surface; therefore, sometimes a cavity is dispensable, as long as, the surface is sufficiently rough for the ectoplacental cone to adhere.
5. Fill the area of the glass microwell with live-imaging culture medium. Make sure to cover the entire silicon setting with the fluid. Due to capillary action, a droplet will be created.
6. Using a pipette transfer the embryo from the dissecting medium to the glass bottom dish filled with live-imaging culture medium.

7. Using forceps, needles (30-gauge) or a combination of both, insert the embryo putting the placental cone through the plastic hole and suspending it. The latero-distal area of the embryo should loosely touch the glass of the dish. This will direct the growth of the embryo avoiding unwanted movement during growth that can lead to an out-of-focus image (Fig. 2.5. B and Fig. 2.5. C).
8. To prevent evaporation of the medium, fill the glass bottom dish with mineral oil. Make sure to cover the entire liquid of the medium.

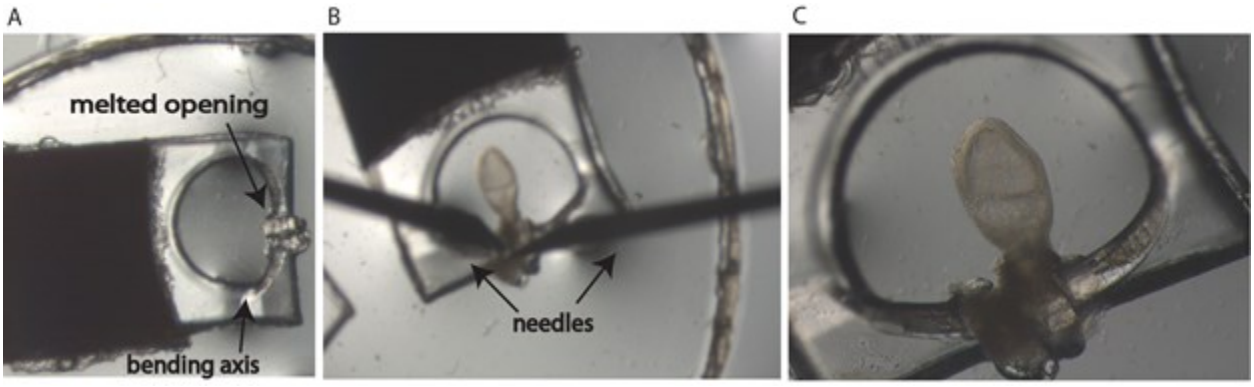

Fig. 2.5. Imaging the lateral regions of the embryo. A) The stage is bent downwards 45°, and prior to adding live-imaging culture medium, an aperture is created using a hot needle. B) With needles and/or forceps, the ectoplacental cone of the embryo is placed through the melted aperture. C) Due to the bending of the plastic, the embryo sits in an angled position, allowing visualization of its lateral areas.

5. Confocal microscopy

1. Pre-warm the confocal microscope and its incubation chambers at least 1 hour prior to imaging. Assure that a temperature of 37°C and 5% CO_2 inside the stage incubator are held constant. The outer incubator is a support to maintain the temperature in the inner chamber at constant. In some machines setting up a higher temperature outside may hold the temperature in the inner chamber, while in other systems setting up the out chamber to 37°C is enough to maintain the inner temperature without fluctuations.
2. Place the mounted sample in the pre-warmed confocal microscope stage (inner) chamber.
3. Look for the region of interest and set the total Z-range wished to image in the embryo. If the embryonic area of interest is bigger than the microscope's field of view, set various xy scanning points to cover the entire area (motorized stage is available in some microscopes).

4. Adjust laser intensity, exposure time, camera gain, and other acquisition parameters. For a sample of 200µm with Z-stack depth of 10-15µm, customize the experiment to an interval of 10 minutes, for 24 hours period.

Imaging analysis.

1. Export the images taken during the experiment with an extension supported by most software programs. Usually, .TIFF is supported by most software. For some types of analysis, like cell tracing, create an extended focus image and then export it.
2. Open the data with Imaris®.
3. Perform cell tracing, measurement, 3D rendering, etc. Other available macros may also be imported and used to analyze the data.

6. Discussion

It is important to emphasize that although mounting the embryo allows visualization of numerous processes, there is a depth limitation due to the opacity and size of the embryo. The depth penetration of spinning disk and swept field confocal microscopes are also limited by the numerical aperture and magnification of the lens. These particular facts make the visualization of deeper processes difficult. In theory, the solution for this problem would be to use a 2-photon confocal microscope known to penetrate to a higher depth; however, we have not assessed the potential of this system. We have noticed this limitation with the imaging of the allantois, where the origin of vascular cells cannot be traced to earlier stages during its formation. Because the allantois is located deeper than the yolk sac, imaging its vascular development is overshadowed by the migration of vascular progenitors located in the latter. Another limitation and requirement of the technique is the use of an inverted microscope. Due to the position of the embryo and the objects that hold it, the lens of the microscope needs to be directly below the sample.

During imaging, loosened cells coming from maternal tissues can be visualized on the surface of the glass. This scenario is almost unavoidable due to the usage of the ectoplacental cone for mounting the embryos; however, trimming the tissue, prior to mounting, can result in less ocular obstruction during imaging.

This technique has been tested with embryonic stages raging from E6.5 to 8.5; however, the technique can be modified to accommodate the needs of other embryonic stages. For example,

the angle of the clear plastic can be increased or decreased for earlier or later stages, respectively (Fig. 2.3. D); another option would be to acquire a lower chamber gasket. To our knowledge, however, the shortest available is 0.8mm deep (the one described here). The same company also produces a higher chamber gasket of 1.3mm that could be used if imaging early organogenesis, for the embryo is larger. Additionally, when using a motorized microscope stage it is possible to image more than one embryo at once. In this paper, we showed the mounting of the embryo utilizing a 35mm diameter petri dish with a glass bottom microwell of 10mm diameter, but 35mm diameter dishes are available from the same company with larger wells. When mounting multiple embryos it is possible to insert ~8-9 embryo stage holders in a 35mm petri dish with a 20mm microwell dish (Fig. 2.7.).

This mounting method has been successfully used to visualize the notochord[88]. Recently, we employed it to image the development of the cardiovascular system in gastrula embryos. Using *Flk-1-GFP* knock-in reporter line, the initial distribution and migration of vascular progenitors was seen (Fig. 2.6.). The tool allows tracing small and large population of cells over a relatively long period of time because a vast region of the embryo is visible under the microscope. Moreover, having a motorized microscope stage allows the visualization of an even larger area, which becomes useful when imaging later stages of gastrulation and early organogenesis, when the embryo size has increased significantly. Other developmental processes of gastrulation and early organogenesis could potentially be studied with this technique. When using high magnifications (e.g. 40x and 60x), observations at the cellular level can also be done; therefore, allowing the study of cell to cell interactions and cellular behavior. We have shown the advantage of using this technique to live-image the distal and lateral sides of the highly dynamic embryo. Cellular behavior and migration has been observed, and tracing has been done to follow cells during a relatively long period of time.

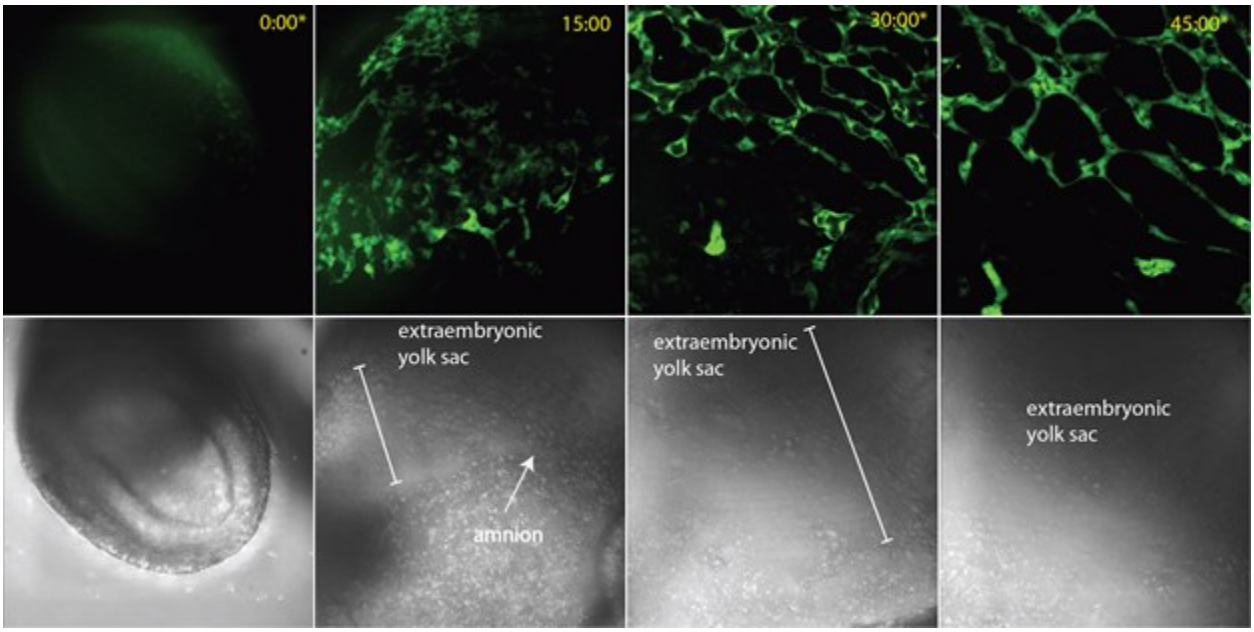

Fig. 2.6. Live-imaging of the development of the yolk sac vasculature in *Flk-1*$^{+/-}$ embryos. Acquisition was performed in E7.5 embryos and lasted for 45 hours without embryonic death. Although the development of the vasculature was delayed, the embryo was able to go from a detached population of cells to an organized honeycomb network of vessels.

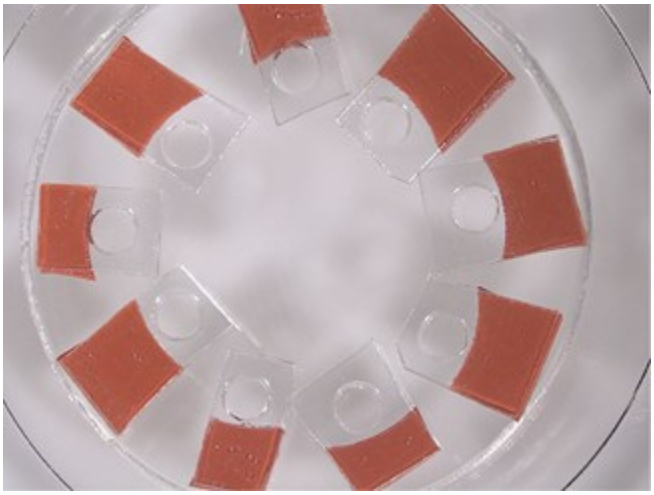

Fig. 2.7. Multiple mounting stages to image more than one embryo in the same experiment. The use of a larger glass microwell (35mm petri dishes) enables the imaging of multiple embryos during the same experiment. For this option to be effective, a microscope with a motorized stage is required.

CHAPTER III

Live-imaging analysis of *Flk-1*-GFP positive cells during gastrulation

Authors: Veronica Sanchez and Yojiro Yamanaka

Manuscript in preparation

1. *Abstract*

Endothelial cells are responsible for formation of embryonic and extraembryonic vasculature. FLK-1/VEGFR2/KDR is one of earliest markers expressed in angioblasts and plays essential roles in its formation. Here, we performed live-imaging analysis of *Flk-1-GFP* gastrula embryos. We identified that angioblasts forming the dorsal aortae are originated from the embryonic-extraembryonic boundary. These cells actively migrate to the embryo midline to form small aggregates that adhere to each other, then forming the luminal structure. We also found that dorsal aortae and endocardium progenitors are found in mutually exclusive areas in the anterior region. In addition, analysis of homozygous *Flk-1* mutant embryos revealed that *Flk-1* is essential for the migration of endothelial progenitors to the embryo and further assembly into vessels although it is dispensable for migration of the mesoderm from the primitive streak.

2. *Introduction*

The cardiovascular system is the first organ to form in vertebrate embryos. Its development is essential for a successful embryogenesis, as other tissues rely on the transport of oxygen and nutrients for proper growth [89]. Endothelial cells are the forming unit of blood vessels and endocardium. Vasculogenesis, the *de-novo* formation of vasculature, occurs in the extramebryonic yolk sac and the embryo proper at around embryonic day (E) 7.0 (reviewed in [41]; [90,91]). Mesodermal cells populated in the extraembryonic region differentiate into angioblasts, endothelial precursors to form the yolk sac vasculature [91] .These *de-novo* formed angioblasts coalesce and form a primitive vascular network called the primary plexus, which is later remodeled into the mature vascular network of the yolk sac. At the same time, within the embryo, endothelial cells contribute to the formation of the primitive streak, the first embryonic vessel, and to the endocardium. The dorsal aortae form in a similar manner as the yolk sac vasculature, when endothelial cells coalesce and form a paired tube that run lateral to the midline. Simultaneously, the endocardium also forms along with the myocardium to generate the primitive heart tube to initiate the embryonic circulation.

Early vascular development is regulated by vascular endothelial growth factor (VEGF). *VegfA*$^{+/-}$ embryos result in embryonic lethality between E11 and E12[46]. These embryos exhibit defective vascularization and reduced number of red blood cells in the yolk sac. VEGF receptors, *Vegfr-1* and *Vegfr-2*, are expressed exclusively in endothelial cells during embryogenesis but have some different functions[92]. Targeted knockout studies have shown that *Vegfr-1*$^{-/-}$mice die in utero between E8.5 and E9.5 [93]. This embryonic lethality is due to formation of excessive number of angioblasts, which results in disorganized high density endothelial cell vessels [44]. *Flk-1/Vegfr2/Kdr,* encoding a receptor tyrosine kinase, is an early mesodermal marker expressing in the mesodermal wing of the mouse gastrula, and it is an essential gene for the development of the vascular and hematopoietic system[45,94]. It mediates cell migration, proliferation and differentiation of angioblast [89]. In the absence of this receptor, mouse embryos die around E9.5 *in utero* due to absence of endothelial and hematopoietic cells, which results in complete lack of vasculature and blood cells [45,94]. In *Flk-1*$^{lacZ/lacZ}$ embryos where the *lacZ* gene is knocked into the *Flk-1* locus, the endocardium is absent, and lacZ+ cells are found in the myocardium[95]. *Flk-1* is highly expressed in angioblasts during vasculature establishment. In adulthood it is only seen in tissue undergoing angiogenesis (vessel sprouting), as it is seen in mammary glands during

pregnancy. High levels of *Flk-1* expression have been linked to neovascularization in cancers[96,97].

In this study, we aimed to identify the origins of cells forming embryonic vasculature, dorsal aortae and endocardium and to characterize dynamic cellular behaviors of angioblast and endothelial cells during vasculogenesis. We performed live-imaging analysis of *Flk-1*-GFP embryos, where *Gfp* is knocked-in to the endogenous *Flk-1* locus during the gastrula stages to trace GFP expressing angioblast and endothelial cells[95]. We found that during the streak stages, *Flk-1*-GFP cells emerged within the nascent mesodermal wings and occupied the extraembryonic yolk sac. In late gastrula stages we found that the dorsal aortae forming cells, located in the embryonic-extraembryonic boundary, strongly upregulated the GFP levels and actively migrated towards the embryo, while an extraembryonic GFP population formed the yolk sac vasculature. We observed characteristic lamellipodia-like protrusions in the migrating dorsal aortae forming cells. From retrospective tracing analysis, we found that cells forming endocardium and dorsal aortae originated from non-overlapping adjacent areas of the anterior cardiac region of the embryo.

Analysis of homozygous *Flk-1* null embryos revealed that FLK-1 is not necessary for the migration of mesodermal cells from the primitive streak, but it is indispensable for the specification and migration of angioblasts from mesodermal cells. Consistent with previous analysis[45], we found GFP+ cells in *Flk-1* null embryos retained in the amnion. Additionally, we identified GFP+ cells within the extraembryonic yolk sac, at the base of the allantois and within the cardiac crescent.

3. Material and Methods

3.1.Embryonic staging

To obtain the right embryonic stage, the mouse mating was timed. Based on the day/night cycle, female mice ovulate close to midnight, and the set up was accordingly performed in the afternoon. The discovery of the plug the morning after mating was considered embryonic stage (E) 0.5 (at 12:00PM). Female pregnant mice were sacrificed by cervical dislocation, and E6.5 or E7.5 embryos were extracted.

3.2.Embryo collection and mounting

Embryos were removed from the decidua at embryonic day (E) 6.5 or 7.5. Dissections were made in a dissection media containing DMEM with phenol red and 10mM solution of HEPES with 5%FBS . The Reichert's membranes were removed and the embryos were mounted to live-image in a media containing 40% DMEM without phenol red, 10% FCS, 50% immediately centrifuged rat serum (heat inactivated), 2 mM GlutaMAX, 1 mM 2-ME, and 1mM sodium pyruvate. Embryos were mounted as per [88].

3.3.Confocal microscopy

In-vivo imaging was collected using Leica DMI6000B with WaveFX spinning disk confocal system and Nikon Eclipse Ti Swept Field confocal. The microscope was equipped with an external incubation chamber as well as a stage incubation chamber to avoid temperature fluctuations. The temperature inside the external incubation chamber as well as the stage incubation chamber was maintained at 37ºC for the entire duration of the experiment. The stage incubator had a gas exchange line, though which 5%CO_2 was administered. We used objectives: 10X NA 0.4 dry, 20X NA 0.7 dry when using Leica and Fluoro 10X NA 0.50 dry and PlanAPO 20X NA 0.75 dry in the Nikon system. The following image settings were used to live-image embryos: for a 24 hour period, z (total range) of ~150 µm with an interval of 10-15µm. The interval acquisition time was set to 10 minutes. When using the swept field technology in the Nikon confocal a slit of 50µm was used. For fixed samples the interval was 10-15µm.

3.4.Retrospective tracing analysis and imaging analysis

Data obtained from the *in-vivo* imaging was analyzed using Imaris®. To identify the origins of *Flk-1*-GFP angioblasts, cells were retrospectively traced.

3.5.Immunofluorescence staining

Immediately after dissecting, embryos were fixed in 2% formaldehyde in PBS for 20 min at room temperature. Embryos were permeabilized with 0.3% Triton X-100 in PBS for 15-30 mins. at room temperature, and blocked in PBS + 0.3% Triton X-100 + 10% Fetal Calf Serum overnight at 4°C. Embryos were then incubated with primary antibodies in blocking solution overnight at 4°C and subsequently, incubated in secondary antibody in blocking solution

overnight at 4C. Finally, the samples were transferred to PBS solution containing nuclear stain and incubated a few minutes at room temperature. Primary antibodies included: anti-Brachury (N-19) goat polyclonal, Santa Cruz Biotechnology. GFP AbFinity recombinant Rabbit monoclonal unconjugated Molecular Probes (Invitrogen).
Secondary antibodies included: Alexa Fluor® 647-conjugated anti-Goat Jackson ImmunoResearch Laboratories (1:400); DyLight^{Tm} 488-conjugated anti-Rabbit Jackson ImmunoResearch Laboratories (1:400).

4. Results

4.1. Flk-1-GFP cells emerge in the mesodermal wing and occupy the embryonic and extraembryonic regions during the streak stages

Mesodermal cells are specified during the epithelial to mesenchymal transition in the primitive streak. *Flk-1*, considered one of the earliest mesodermal markers, is first detected at the mid-streak stage in the proximal posterior regions of the embryo[95]. Immunostaining data from mid to late streak embryos showed FLK-1 protein expressing cells within the extraembryonic region [90]. To characterize the emergence and behavior of *Flk-1* positive cells during the streak stages, we performed live-imaging analysis using the *Flk-1*-GFP mouse line, which has the *GFP* gene knocked into one of the *Flk-1* locus[95].

Flk1-GFP+ cells became visible at the early to mid-streak stage (staging according to [98]), and localized around the embryonic-extraembryonic boundary laterally to the primitive streak (Fig. 3.1A, time 0:00). Within the first hour of imaging, new *GFP* positive cells emerged within the embryonic region, occupying the nascent mesodermal wing. As consistent with a previous study[99], no *FLk-1*-GFP+ cells were identified within the primitive streak at the streak stages.

During the early and mid-streak stages, a continuous emergence of *Flk-1*-GFP cells was observed. The GFP+ population started to expand both vertically and horizontally along with embryo growth (Fig. 3.1A time 0:00-4:00). At the same time, GFP+ cells initially located in the embryonic-extraembryonic boundary started to actively migrate towards the extraembryonic region. These migrating cells displayed lamellipodia-like protrusions (Fig. 3.1 B box). After 4 hours of imaging, while more GFP+ cells emerged in the mesodermal wing, GFP+ cells started to migrate laterally. By the late streak stage (12 hours after imaging), GFP+ cells were in the mesodermal wings in the embryonic region as well as in most of the extraembryonic region (Fig.

3.1B). During the course of imaging, no GFP+ cell was found within the primitive streak or the epiblast. To further investigate the absence of *Flk-1*-GFP+ cell from the primitive streak, we used immunohistochemistry with antibodies against GFP and Brachyury, a marker of the primitive streak. No GFP+ cell co-localized with any Brachyury positive cell, confirming the absence of *Flk-1*-GFP in the primitive streak (Fig. 3.1C).

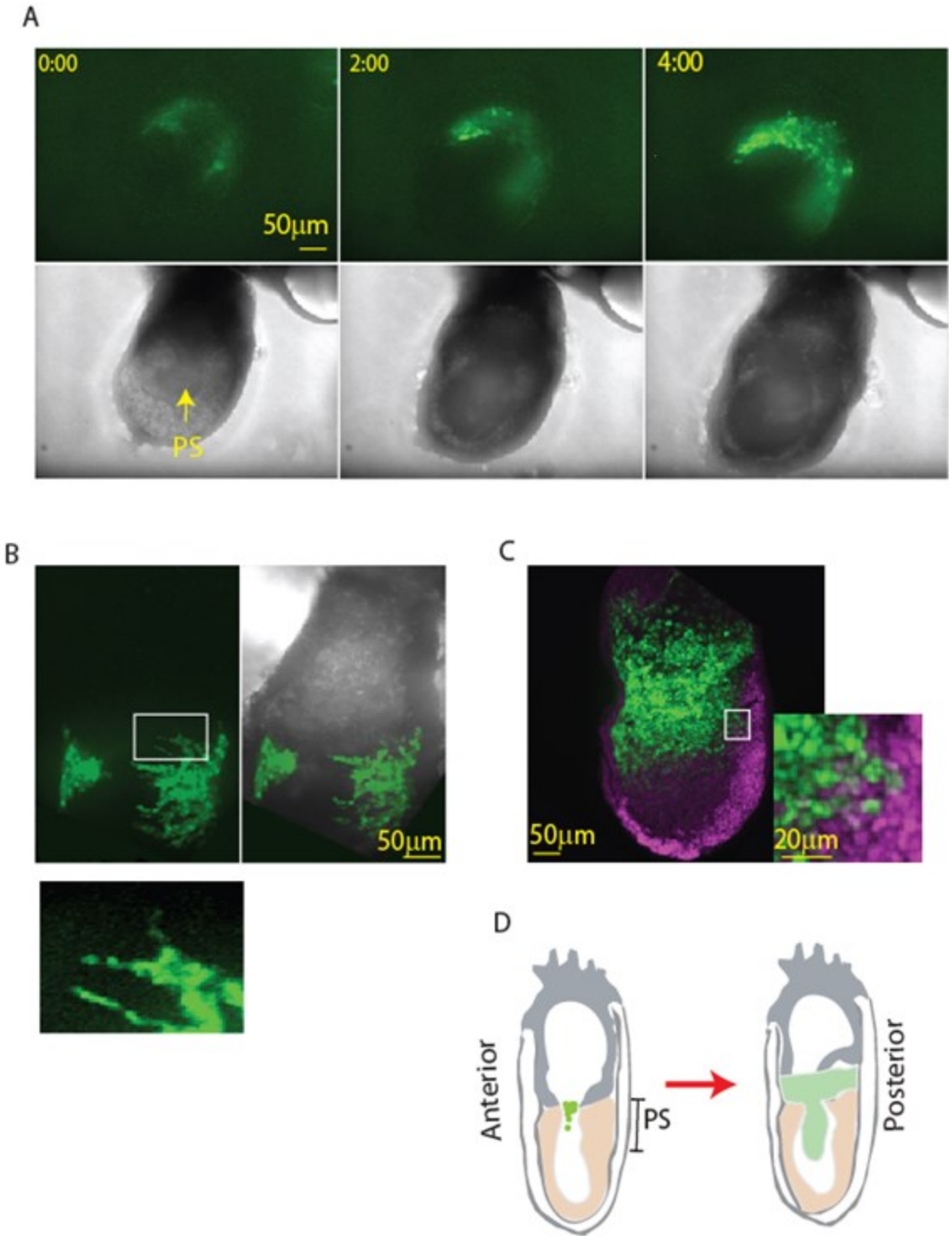

Fig. 3.1. Time-lapse imaging of FLk-1-GFP distribution during the streak stages reveals the presence of *Flk-1*-GFP positive cells in the embryonic and extraembryonic regions. A) Posterior view of an E6.75 embryo showing initial detection of the GFP signal in the embryonic, and boundary areas, and further detection after several hours of imaging. Rendering of GFP

images (top), and rendered DIC images overlaid on GFP images (bottom). Time 0:00 indicates hr:min, from mid streak to pre-late streak stage (time 0:00-4:00). B) Lateral view of a different embryo during the streak stage showing the pattern of *Flk-1*-GFP+ cells. An asterisk indicates embryonic-extraembryonic boundary. C) Immunostaining of an embryo during the no bud stage showing the absence of *Flk-1*-GFP+ cells from the primitive streak (green GFP; purple Bra). D) Lateral schematic representation of the distribution of *Flk-1*-GFP cells (in green) from the middle streak stage to the late streak stage. PS-primitive streak.

4.2 *Flk-1-GFP cells at the embryonic-extraembryonic boundary actively migrate toward the embryonic region to form the primitive streak*

Embryonic and extraembryonic vasculogenesis take place with the formation of the blood island in the extraembryonic yolk sac and assembly of vessels from angioblasts [100]. Flk-1 is expressed in endothelial angioblasts forming the embryonic vasculature, like the primitive streak, the first embryonic blood vessel [90,101]. However, the exact origin of these cells has not been fully identified. The process of dorsal aortae formation in micewas carefully analyzed using confocal microscopy and electron microscopy on static fixed embryos[102]. Although this work provided a foundation of molecular mechanisms for dorsal aortae formation, the dynamic process has not been visualized in live embryos. To identify the origin of dorsal aortae forming cells and visualize the process of tube formation in the embryo, we performed live-imaging analysis from the early allantois bud to the 2-4 somite stage.

From the early to late bud stages, *Flk-1*-GFP+ cells were located in the extraembryonic and embryonic region, and close to the boundary (Fig. 3.2A and 2B). At the early head-fold stage some embryonic GFP+ cells near the boundary upregulated GFP and actively migrated towards the embryo midline while the rest of GFP+ population stayed (Fig. 3.2B time 0:00-15:00 and Fig. 3.2C yellow dots *vs.* red dots).

During migration, these GFP+ cells showed dynamic cellular interactions, repeatedly attaching and detaching to each other (Fig. 3.2C; yellow arrow). Moreover, while migrating, the cells elongated (Fig. 3.2C).

At the 1-2 somite stage, migrating GFP cells reached a zone adjacent to the embryonic midline, stopped migrating and aligned parallel to the midline (Fig. 3.2E). This arrangement formed a

rudimentary chord like structure that contained small luminal regions (Fig. 3.2E right panel). As the dorsal aortae remodeled into a tube-like structure more GFP+ cells adhered to the forming tube.

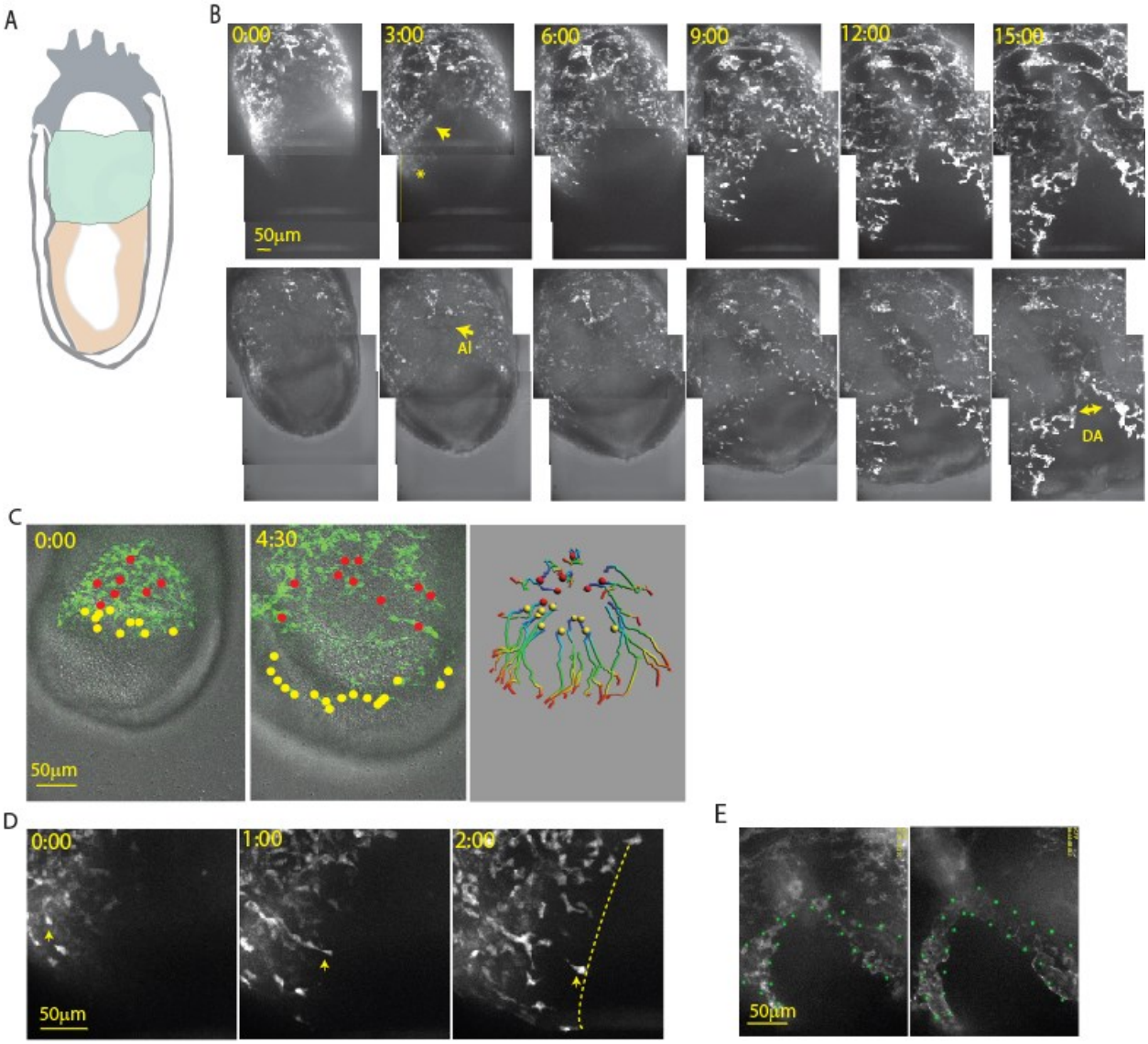

Fig. 3.2. A subpopulation of *Flk-1*-GFP cell actively migrate from the boundary to form the DA. A) Schematic representation of the localization of *Flk-1*-GFP+ cells during the no bud stage (embryo shown in lateral view). *Flk-1*-GFP cells are found in the extraembryonic regions and nearby the embryonic extraembryonic boundary. B) Posterior view of an E7.5 embryo from the early allantois bud until 1-2 somite stage. Dorsal aortae progenitors are located in the embryonic-extraembryonic (emb-exe) boundary (arrow time 3:00). Time 9:00, GFP+ cells

migrate to the midline, coalesce and form the dorsal aortae (times 12:00-15:00), Top images show GFP only, bottom images display GFP on top of DIC for better contrast of the position of the cells. C) Origin of dorsal aortae and yolk sac vasculture angioblasts. Dorsal aortae progenitors shown in yellow dots are located near the embryonic-extraembryonic boundary, while yolk sac angioblasts are located extraembryonically (red dots). Right panel shows the migration tracks of angioblasts. Notice how dorsal aortae progenitors display distal movement while yolk sac angioblasts display lateral ones. D). Elongation of a dorsal aortae progenitors while migrating (arrow; dashed line indicates the dorsal aortae formation site). E) Posterior view of an embryo showing the dorsal aortae (green dots) formed after migration of the angioblasts.

4.3 *Endocardium and the dorsal aortae are originated from Flk-1-GFP+ cells in different areas of the gastrula embryo*

In vitro differentiation studies suggest that multipotent FLK-1 positive mesodermal cells can generate the endocardium and myocardium as well as smooth muscle, endothelial, and hematopoietic lineages [103-107]. Next, we analyzed GFP+ cells in the anterior area of the embryos to visualize the cardiovascular formation.

As described earlier, dorsal aortae progenitors upregulated GFP, and after three hours, at the early head-fold stage, actively migrated towards the anterior embryonic midline (Fig. 3.3 A purple dots; Fig. 3.3B time 0:00-3:00). The characteristics of these migrations were similar to that described in the previous section. As the dorsal aortae progenitors migrated, endocardial GFP+ cells located at the most anterior region, started to join at the anterior midline, creating an arch-like morphology (Fig. 3.3A and 3.3B yellow dots). As the dorsal aortae were being formed, its proximal side connected with endocardium progenitors (Fig. 3.3B time 9:00 white box). Along with the formation of the foregut pocket (2-4 somite stage), the connection of dorsal aortae and endocardium was placed behind the pocket to generate the primary heart tube. During the early somite formation, *Flk-1*-GFP cardiac mesoderm further converged at the midline of the embryo generating the elongated primary heart tube (Fig. 3.3D).

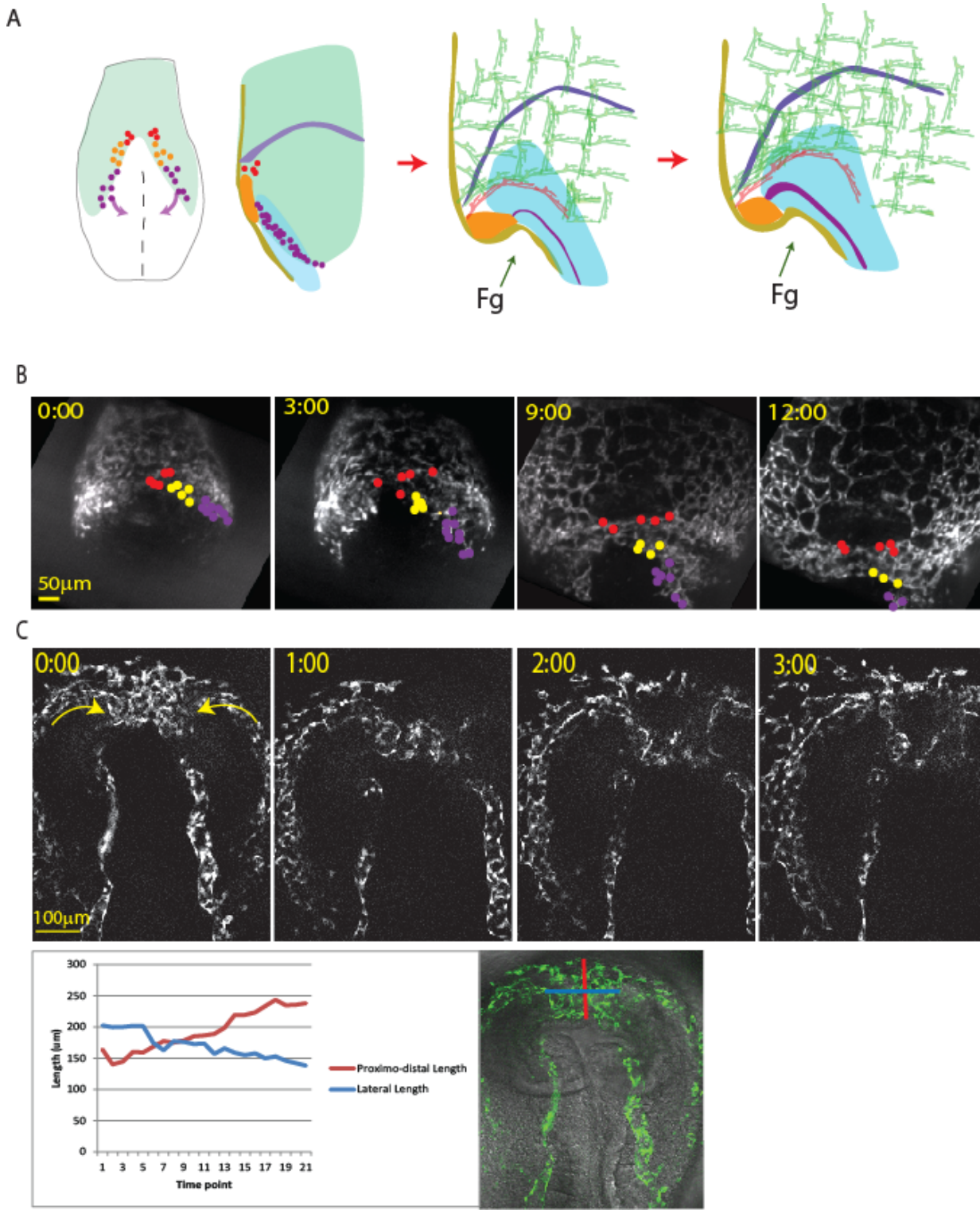
A
Fg
Fg
B
0:00
3:00
9:00
12:00
50µm
C
0:00
1:00
2:00
3:00
100µm
300
250
200
150
100
50
0
Length (µm)
1 3 5 7 9 11 13 15 17 19 21
Time point
Proximo-distal Length
Lateral Length

Fig. 3.3. In the anterior region, DA progenitors migrate while cardiac mesoderm converges at the midline to form the heart tube. A) Cartoon representation of the fate of *Flk-1*-GFP cells in the anterior area of an E7.5 embryo (purple dots= dorsal aortae forming cells, yellow= cardiac mesoderm, red= cardinal vein forming cells). B) The anterior view of an E7.5 embryo showing the contribution of *Flk-1*-GFP+ cells to the embryonic vasculature. Dorsal aortae and cardiac *Flk-1*-GFP+ progenitors are located near the emb-exe boundary (time 0:00 purple and yellow dots). As the foregut (Fg) forms and the dorsal aortae progenitors migrate, cardiac progenitors join at the midline of the embryo (time 3:00-9:00; white box indicates dorsal aortae connection to cardiac mesoderm). C) Conversion of *Flk-1*-GFP+ cardiac mesoderm in the midline to form the heart tube (yellow arrow).

4.4. *Formation of an avascular area in the anterior extraembryonic yolk sac*

During our live-imaging analysis of the anterior region of the embryo, we noticed an avascular area in the anterior yolk sac adjacent to the primitive heart tube (Fig. 3.4). At the late bud stage, *Flk-1-GFP*+ cells were distributed evenly in the most anterior tip of the embryo (Fig. 3.4 time 3:00). As the embryo underwent vasculogenesis, an avascular area proximal to the cardiac mesoderm emerged. Inside the avascular zone some low *Flk-1*-GFP+ cells were present and started to migrate away from the zone to become part of the yolk sac vasculature (Fig. 3.4 bottom panels, yellow dots).

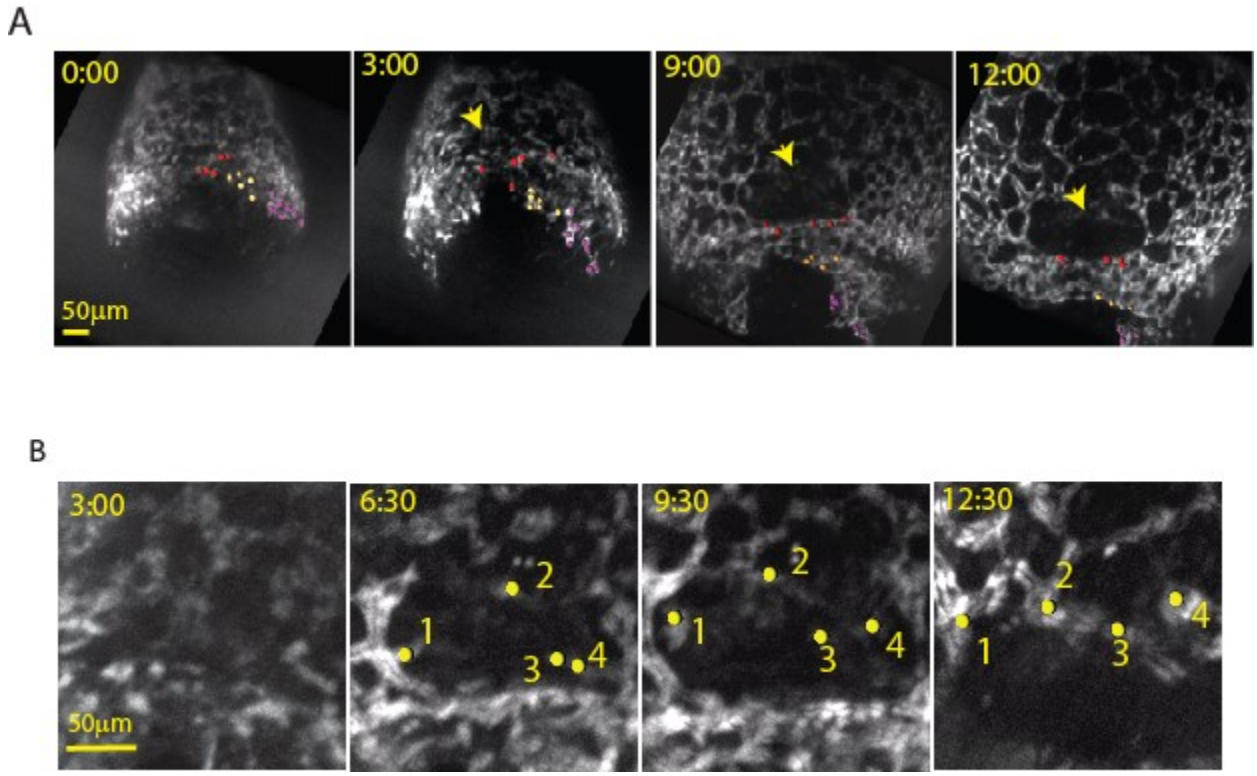

Fig. 3.4. Formation of the avascular zone in the anterior extraembryonic region. Top panels (time 0:00-12:00) show the formation of the avascular zone (yellow arrow) in respect to the embryo, where cells appear to be present throughout the entire embryo at the beginning (time 0:00-3:00) and then absent themselves from the area proximal to the forming heart (time 9:00-12:00). Bottom panels: Cells within the avascular forming zone do not upregulate GFP and migrate away from the area to become part of the yolk sac vasculature (Bottom panels yellow dots time 6:30-12:30). Time differs between top and bottom panels to better show specific events during the process.

4.*5 Vasculogenesis in the yolk sac is achieved by multiple extensions and connections between angioblasts*

The yolk sac is a highly vascularized extraembryonic tissue. The majority of the *Flk1*-GFP+ cells that migrate into the extraembryonic region become the yolk sac vasculature. Various publications have suggested that vasculogenesis starts prior to the embryonic vasculogenesis[93], with the accumulation of mesodermal cells in the extraembryonic yolk sac during the streak stages.

At the late streak stage and early no bud stage, the extraembryonic region was occupied by *Flk-1*-GFP+ cells that had no contact with each other (Fig. 3.5 time 0:00). As the embryo developed towards the late bud stage (during the first hours of imaging), GFP was upregulated and the cells started to display small lamellipodia-like projections in random directions (data not shown) while migrating short distances (Fig 3.5). They established cell contact between nearby cells to form small luminal aggregates (Fig. 3.5 time 4:00). By the 1-4 somite stage, the primary vascular network in the yolk sac was established and the subsequent vascular remodeling was observed.

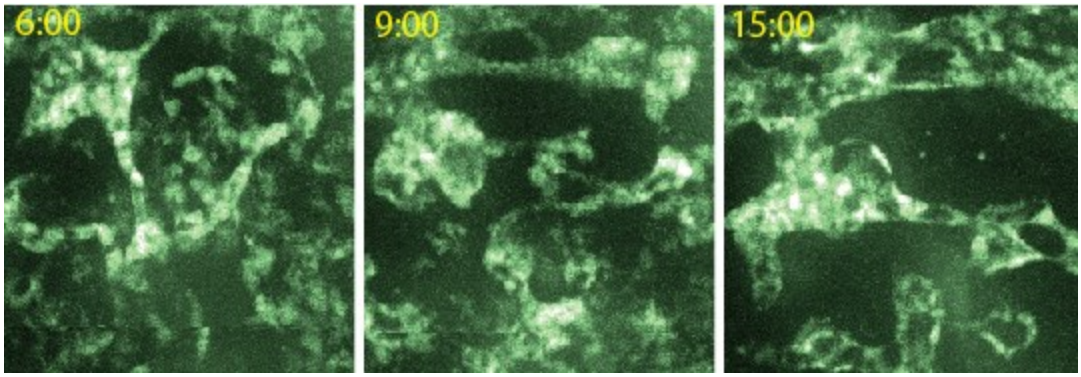

Fig. 3.5 Time-lapse imaging of the vasculogenesis in the extraembryonic region. At time 0:00 (no bud stage) the cells are spread throughout the extraembryonic region. No cell-cell contact is established at this time. The cells make small movements and adhere to each other forming a disorganized plexus (time 4:00) that later remodels into a network (time 12:00). The arrow indicates a cell making small movements and displaying protrusion while doing it.

4.6 *Flk-1 is dispensable for early mesoderm migration from the primitive streak but necessary for specification and migration of endothelial cells.*

Chimeric analysis of *Flk1-/-* cells in wild type embryos showed that *Flk-1* is cell autonomously required to become endothelial cells [45]. *Flk-1* null cells in chimeric embryos are excluded from the cardiovascular system and localized to the amnion, suggesting migration defects in *Flk-1* mutant cells. We examined this mislocalization directly by tracing *Flk-1*-GFP cells in *Flk-1*$^{GFP/GFP}$ mutant embryos.

At the early streak stage, GFP cells in *Flk-1*$^{GFP/GFP}$ null embryos were detected in the nascent mesodermal wing, extraembryonic mesoderm, and at the embryonic-extraembryonic boundary. We did not find any difference in distribution and behavior of the GFP cells in mutant embryos

compared to GFP cells in heterozygous embryos during the streak stages. These results suggest that FLK-1 function is not required for the early migration of mesodermal cells from the primitive streak.

By the late he-d fold stage, many GFP cells accumulated at the base of the allantois (Figure 3.6A, 4:00-12:00 asterisk denotes base of allantois). Consistent with the previous studies [45,94], accumulation of *Flk-1*-GFP+ cells was seen at the level of the amnion (Fig. 3.6 A time 12:00 arrow). The cells emerged in the area and no migration was seen.

In contrast to heterozygous embryos, at the late bud to the early head-fold stage no GFP upregulation was seen in mutant embryos; instead, the cells gradually downregulated GFP. These weak GFP+ cells did not migrate and had a round morphology without lamellipodia-like protrusions (Fig. 3.6B). These results suggest that *Flk-1 is* required for angioblast/endothelial cell specification. Without *Flk-1*, these cells became extraembryonic yolk sac and amnion mesoderm.

In the anterior region, some weak GFP+ cells were distributed within the cardiac crescent (Fig. 3.6C). By the head-fold stages, the GFP cells started to disperse giving rise to a hollow shape corresponding to an endocardium-less heart tube (Fig. 3.6E). Twelve hours after culture, the structure started showing coordinated myocardium contractions. Additionally, no vascular structure was formed in null embryos.

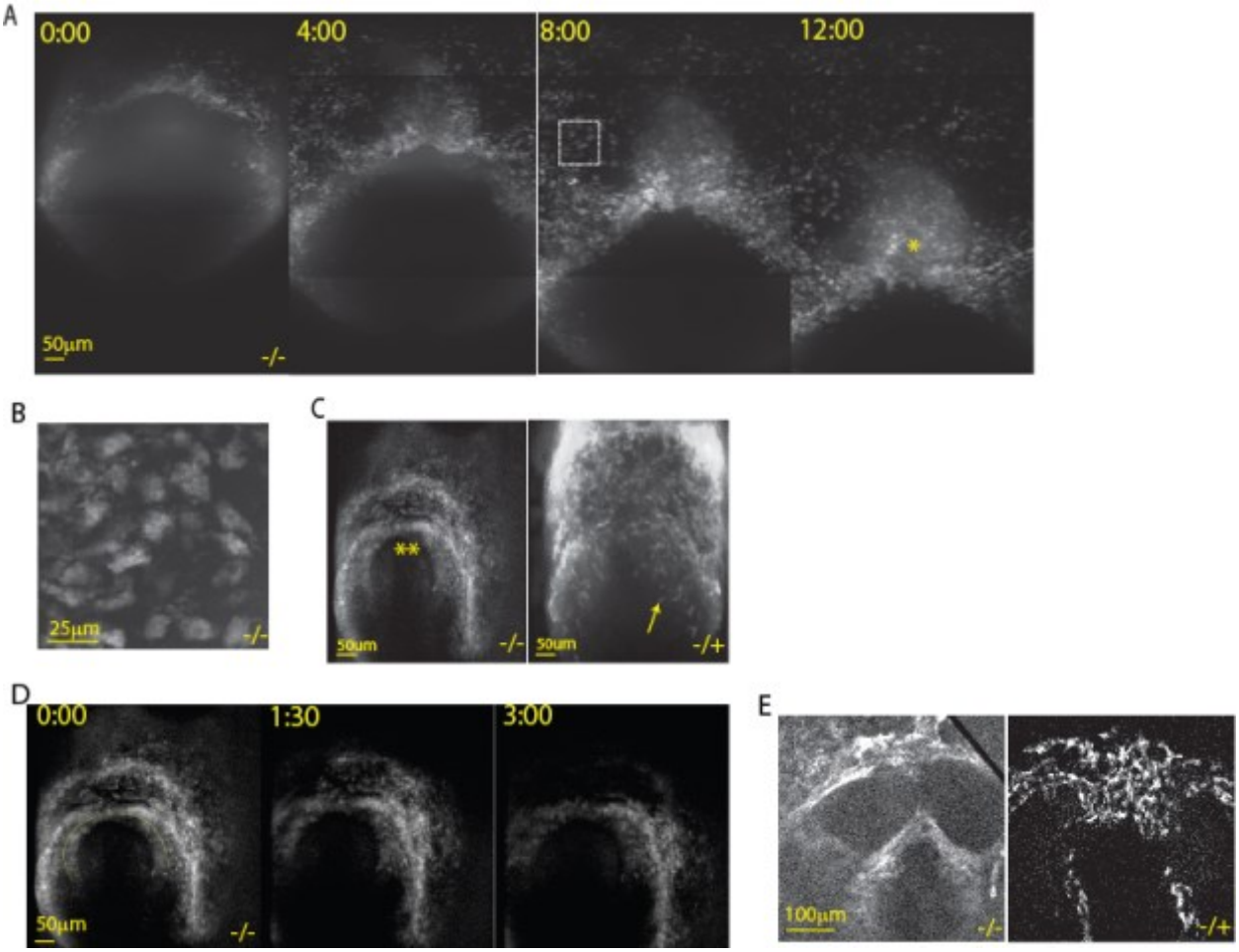

Fig. 3.6. Time-lapse imaging of *Flk-1*$^{GFP/GFP}$ embryos during the head-fold stages reveals Flk-1 is necessary for migration of angioblast and assembly into vascular lumens. A) Posterior side of an E7.5 homozygous *Flk-1*-GFP embryo. During the allantois bud stages, cells are found in the embryonic and extraembryonic region (time 0:00). No active migration or cell movement was observed. GFP cells accumulated in the amnion and at the base of the allantois. B) GFP cells also remained present in the extraembryonic region and displayed a round shape, with no visible lamellipodia. C) Anterior side of a homozygous *Flk-1*-GFP embryo compared to a heterozygous (right panel) of similar developmental stage (** denotes cardiac mesoderm; arrow- DA progenitors) GFP positive cells can be observed as part of the cardiac mesoderm in *Flk-1*$^{GFP/GFP}$ and *Flk-1*$^{GFP/+}$ embryo. D) Time lapse imaging showed no migration was made by DA progenitor, although the cardiac crescent was able to form (time 0:00-3:00). E) *Flk-1*-GFP cardiac mesoderm were able to converge at the midline and form a heart tube, however the endocardium was never formed (compare the left panel corresponding to a homozygous embryo

with the right panel corresponding to a heterozygous embryo- no *Flk-1*-GFP cell was found within the inner area of the heart tube).

5. Discussion

Through the use of live-imaging analsis we have studied the distribution and behavior of mesodermal cells marked by *Flk-1*-GFP expression. *Flk-1* has been implicated as a marker for lateral plate mesoderm and in the specification of endothelial and hematopoietic cells, as well as in the development of the endocardium and myocardium[94].

Flk-1 and migration

Our tracing analysis showed that the contribution of *Flk-1*-GFP cells to extraembryonic yolk sac, to the dorsal aortae and the endocardium. As previously reported, *Flk-1*-GFP cells became detectable at the early streak stage but were absent from the primitive streak[95]. We confirmed these results with Brachyury antibody staining using Brachyury, a T-box transcriptional factor expressed throughout this structure during gastrulation. Chimeric studies with *Brachyury*-null ES cells and wild type embryos demonstrated the importance of this gene for the movement of mesoderm from the primitive streak [108]. In *in-vitro* studies using *Bra-GFP* ES cells a subpopulation of Bra^{+} mesodermal cells also become positive for $FLK\text{-}1^{+}$[109]. Contrary to the *in-vitro* studies, during our live-imaging analysis *Flk-1*-GFP+ cells were detected at the lateral sides of the primitive streak, never within. However, we do not rule out the possibility that during early gastrulation *Flk-1*-GFP levels are too low to be detected within the primitive streak, or, conversely, that the number of cells expressing GFP is too low to be captured by the microscope camera.

Previous studies have demonstrated the essential role of *Flk-1* for endothelial migration during vasculogenesis [45,110]. Our mutant analysis indicates that *Flk-1* is dispensable for the migration of *Flk-1*-GFP+ cells from the primitive streak. Mutant embryos showed a similar pattern of migration and colonization of the embryo, compared to that in heterozygotes. *Flk-1*, however, becomes crucial during the migration of angioblasts to form the dorsal aortae and yolk sac vasculature. At the end of the streak stages, *Flk-1*-GFP+ cells appeared in the correct position within the mesodermal wing. During the allantois bud stage, $Flk\text{-}1^{GFP/GFP}$ cells were found in the

embryonic extraembryonic boundary; however, lack of upregulation of *Flk-1* appeared to result in the lack of migration in angioblasts.

What exactly provokes angioblasts to migrate to the embryo remains disputable. Early studies in chicks showed that endothelial cells never crossed the embryonic midline [111]. Moreover, the mutant embryos' floating head and no tail, which lacks notochords, failed to form the dorsal aortae [112]. The results pointed to the notochord as the signaling center. VEGF, a ligand of FLK-1 has been proposed as a possible chemoattractant expressed as a gradient from the hypochord in *Xenopus;* however, this idea has proven to be difficult to prove in mammals because of the inexistence of this structure. It has also been found that an existing gradient of VEGF in the retina is required for the generation of filopodia and therefore migration. In this model, expression of *Flk-1* is enriched in the filopodia, which promotes cell migration towards the VEGF source [113]. Real time PCR and immunohistochemistry analysis showed that *VEGF-A* is expressed with more strength in the anterior side of the embryo, while *Flk-1* expression is stronger in the posterior region at E7.5-E7.75[114]. *In-vitro*, FLK-1 positive cells migrated towards a VEGF source. FLK-1 ligands PLGF and VEGF-E were also able to produce a migratory effect, but to a lesser degree [114]. Moreover, removal of *Vegf-A* or *Flk-1* from the floor plate results axon guidance defects[115].

In recent years, some focus has been given to axon guidance molecules. That is the case with Sema3E, of the semaphorin family, which has been proven to act as a repulsive cue coming from the LPM and the notochord to sculpt and correctly position angioblasts to form the dorsal aortae in an avascular zone[40]. Such avascular zone between the dorsal aortae and the yolk sac vasculature disappears in the absence of *Sema3E*[40].

Taking these data together with our results leads to the idea that a source of *Vegf-A*, which creates a gradient, could be coming from the notochord. At E7.5, when the angioblast are found in the embryonic-extraembryonic boundary and all the way to the extraembryonic region, the *Vegf-A* gradient could be sufficient to attract the cells at the boundary, producing migration towards the notochord. Then repelling signals, like Sema3E, would act to correctly made and position the dorsal aortae, thus creating an avascular zone between the dorsal aortae and yolk sac vasculature.

Origins of the dorsal aortae angioblasts

The dorsal aortae are formed as paired tubes during gastrulation by endothelial cells. Later in development the tubes will fuse in the midline and will become the descending aorta, the largest blood vessel in the trunk[40]. The anterior end of the dorsal aortae is connected to the heart by the outflow tract and the posterior is connected to the vascular plexus in the splanchnic mesoderm. Live-imaging analysis of Cy3-QH1 quail embryos demonstrated that endothelial cells migrate from a region within the lateral plate and form the primitive streak[116]. In the murine embryo, the exact origin of the dorsal aortae progenitors remained unclear. Our study clearly answered the standing question about the origins of the endothelial cells forming the primitive streak. We identify endothelial cells coming from a region near the embryonic extraembryonic boundary that contributed to the dorsal aortae formation.

Tube formation

Proper embryonic development depends in part on the correct establishment of the vascular system, as tubes are responsible for the transport of nutrients and gasses. During blood vessel development, endothelial cells are the only cells capable of forming luminal vascular tubes[102]. Previous studies have come up with two different ideas about how blood vessels developed. Early ideas, resulting from studies of zebrafish, proposed that large intracellular vacuoles developed in endothelial cells and later coalesced with other vacuoles from adjacent endothelial cells, therefore forming a tube [117]. However, a more recent study described in greater detail the development of the primitive streak. In it, it was concluded that endothelial cells assemble into a cord before forming a central vascular lumen[102]. Additionally, the authors suggested that the vascular lumen development at the cell-cell contact between adjacent cells where no vacuoles are observed. During our live-imaging analysis, however, angioblasts start migrating as separate cells but soon after, they start adhering with each other to form small aggregates that start to display disorganized but dynamic rearrangements that appear to form luminal structures. If this is the case then, the dorsal aortae form by the adhesion of small luminal structures. The tube becomes connected with the addition of new joining cells.

Contribution of Flk-1-GFP+ cells to the cardiac lineages

Some studies suggest the existence of a multipotent FLK-1 expressing progenitor giving rise to cardiac and vascular lineages[106,107]. Our tracing analysis showed that only *Flk-1*-GFP+ cells in

the anterior region of the embryo contribute to the endocardium, while the GFP+ cells adjacent to both lateral sides contributed to the dorsal aortae.

During the cardiac crescent formation, a group of cells located laterally did not contribute to the endocardium formation. Moreover, they did not appear to be making contact with the cells forming the endocardium or with dorsal aortae progenitors. It is unclear what these cells will contribute to, but we speculate that they may contribute to the heart later in development, since different waves of cardiac progenitors are known to migrate later in heart development[118].

CHAPTER IV

Conclusions and Future experiments

The *in-vivo* imaging of gastrula embryos is difficult because of their shape. With the techniques developed in the laboratory, however, we were able to successfully image the development of the cardiovascular system. The technique allows the imaging of the embryo for prolonged periods of time because it minimizes damage to the embryo and diminishing its movements. More specifically, during my project it was used to live-image *Flk-1*-GFP cells from its early detection, at E6.5, until their contribution to the cardiovascular system. Due to the advantage of live-imaging, we were able to trace the origins of the dorsal aortae progenitor, previously unknown. Moreover, the behavior of *Flk-1*-GFP cells was also studied with the aid of this technique, something not possible when utilizing other tools like immunohistochemistry or in-situ hybridization, because the embryo is fixed.

Although we were able to observe the overall behavior of *Flk-1*-GFP cells, during our analysis we observed weak GFP populations located distally to the dorsal aortae progenitors. As active migration from dorsal aortae progenitors occurred, these populations further downregulated GFP, becoming untraceable. We hypothesize that cells within the weak GFP population will contribute to other structures forming within the embryo. This assumption is based in the fact that *Flk-1* is an early general mesodermal marker expressed within the LPM. In fact, *in-vitro* studies have shown multipotent FLK-1-positive cells capable of differentiating in different lineages, including cardiac, hematopoietic, vascular and muscular lineages. We predict that during early mesodermal specification *Flk-1* marks multipotent mesodermal cells that will later be specified and contribute to other non-endothelial derived structures. For this part of the study, our goal is to identify the contribution of these weak GFP cells in the embryo.

It is intended to use FLK-1 as a marker to create a fate map of the LPM to further address the fate of weak *Flk-1*-GFP-cells. Through the use of homologous recombination, *iCre* will be inserted in the *Flk-1* endogenous locus. We have created a plasmid containing *iCre* and are in the process of inserting it into a bacterial artificial chromosome (BAC). The BAC contains *Flk-1* genomic region, in which our sequence of interest, iCre, will be inserted in exon 1 upstream of the start site. The BAC will be used to insert *iCre-ERT2* to the genome in the *Flk-1* locus. The reason for using improved (Cre recombinase) iCre instead of the regular Cre recombinase is because the latter comes from a prokaryote source and its codon usage in eukaryotes is not

optimal. Moreover, it contains CpG dinucleotide repeats, which can lead to epigenetic silencing during mammalian development. iCre was developed to counteract these problems by inserting silent mutations in the original *Cre* gene. Moreover, the iCre technology allows a better detection of weakly expressed genes within cells[119].

Upon establishment of the *Flk-1-iCre* mouse line, a cross will be made with Rosa-CAG-Loxp-Stop-Loxp-tdTomato mouse line to generate double heterozygous embryos carrying Flk-1-iCre::Rosa-CAG-Loxp-Stop-Loxp-tdTomato. The result will be an embryo in which the Flk-1 population is marked by tdTomato and displays the dynamics seen in wildtype Flk-1 cells, but Flk-1 downregulated populations will be marked as well.

CHAPTER V

Annex

Animalcare Rgo

Acciones

Para: Veronica Sanchez

Inbox

jueves, 11 de agosto de 2011 10:10 a.m.

Hello Veronica Sanchez,

You have successfully passed the test for the ADVANCED LEVEL of the McGill University Animal Care Committee Theory Training Course.

* * * Your grade is 100 %.* * *

You are now certified until **August of 2016**. Your name will be entered in our database.
Certificates will no longer be issued by internal mail.
Your training information is entered in the McGill Training database and the receiving of certificates does not affect protocol approval.

If you require a certificate as proof of training for another university or facility, you may request an electronic version (as valid as the originals) through Animalcare Rgo animalcare@mcgill.ca and it will be sent to you.

Animalcare Rgo

Acciones

Para: Veronica Sanchez; Yojiro Yamanaka, Dr

Inbox

jueves, 11 de agosto de 2011 02:51 p.m.

Hello Dr. Yamanaka,

I am pleased to inform you that all the training requirements for the Amendment to AUP 5851 have been completed. Veronica Sanchez has completed the Theory Course and has registered to the appropriate practical training workshop(s). The Amendment has been stamped "Training Approved" and submitted to Claude Lalande (Assistant Director - Animal Compliance) for final approval.

REFERENCES

1 Tam, P. P. L. & Behringer, R. R. Mouse gastrulation: the formation of a mammalian body plan. *Mechanisms of Development* **68**, 3-25, doi:10.1016/s0925-4773(97)00123-8 (1997).

2 Mikawa, T., Poh, A. M., Kelly, K. A., Ishii, Y. & Reese, D. E. Induction and patterning of the primitive streak, an organizing center of gastrulation in the amniote. *Developmental Dynamics* **229**, 422-432, doi:10.1002/dvdy.10458 (2004).

3 Stern, C. D. Mesoderm induction and development of the embryonic axis in amniotes. *Trends in Genetics* **8**, 158-163, doi:10.1016/0168-9525(92)90217-r (1992).

4 Kimelman, D. Mesoderm induction: from caps to chips. *Nature Reviews Genetics* **7**, 360-372, doi:10.1038/nrg1837 (2006).

5 Beddington, R. S. & Smith, J. C. Control of vertebrate gastrulation: inducing signals and responding genes. *Current opinion in genetics & development* **3**, 655-661, doi:10.1016/0959-437x(93)90103-v (1993).

6 Faust, C. & Magnuson, T. Genetic control of gastrulation in the mouse. *Current opinion in genetics & development* **3**, 491-498, doi:10.1016/0959-437x(93)90125-9 (1993).

7 Hamburger, V. & Hamilton, H. L. A series of normal stages in the development of the chick embryo. *Journal of Morphology* **88**, 49-&, doi:10.1002/jmor.1050880104 (1951).

8 Khaner, O. & Eyalgiladi, H. The embryo-forming potency of the posterior marginal zone in stage-x through stage-xii of the chick. *Developmental Biology* **115**, 275-281, doi:10.1016/0012-1606(86)90248-4 (1986).

9 Acloque, H., Adams, M. S., Fishwick, K., Bronner-Fraser, M. & Angela Nieto, M. Epithelial-mesenchymal transitions: the importance of changing cell state in development and disease. *Journal of Clinical Investigation* **119**, 1438-1449, doi:10.1172/jci38019 (2009).

10 Arnold, S. J. & Robertson, E. J. Making a commitment: cell lineage allocation and axis patterning in the early mouse embryo. *Nature Reviews Molecular Cell Biology* **10**, 91-103, doi:10.1038/nrm2618 (2009).

11 Chuai, M. & Weijer, C. J. Who moves whom during primitive streak formation in the chick embryo. *Hfsp Journal* **3**, 71-76, doi:10.2976/1.3103933 (2009).

12 Ciruna, B. & Rossant, J. FGF signaling regulates mesoderm cell fate specification and morphogenetic movement at the primitive streak. *Developmental Cell* **1**, 37-49, doi:10.1016/s1534-5807(01)00017-x (2001).

13 Mathieu, J. *et al.* Nodal and Fgf pathways interact through a positive regulatory loop and synergize to maintain mesodermal cell populations. *Development* **131**, 629-641, doi:10.1242/dev.00964 (2004).

14 Skromne, I. & Stern, C. D. Interactions between Wnt and Vg1 signalling pathways initiate primitive streak formation in the chick embryo. *Development* **128**, 2915-2927 (2001).

15 Mitrani, E., Gruenbaum, Y., Shohat, H. & Ziv, T. Fibroblast growth-factor during mesoderm induction in the early chick-embryo. *Development* **109**, 387-393 (1990).

16 Seleiro, E. A. P., Connolly, D. J. & Cooke, J. Early developmental expression and experimental axis determination by the chicken Vg1 gene. *Current Biology* **6**, 1476-1486, doi:10.1016/s0960-9822(96)00752-x (1996).

17 Hume, C. R. & Dodd, J. Cwnt-8c - a novel wnt gene with a potential role in primitive streak formation and hindbrain organization. *Development* **119**, 1147-1160 (1993).

18 Streit, A. & Stern, C. D. Establishment and maintenance of the border of the neural plate in the chick: involvement of FGF and BMP activity. *Mechanisms of Development* **82**, 51-66, doi:10.1016/s0925-4773(99)00013-1 (1999).

19 Bertocchini, F. & Stern, C. D. The hypoblast of the chick embryo positions the primitive streak by antagonizing nodal signaling. *Developmental Cell* **3**, 735-744, doi:10.1016/s1534-5807(02)00318-0 (2002).
20 Zhou, X. L., Sasaki, H., Lowe, L., Hogan, B. L. M. & Kuehn, M. R. Nodal is a novel tgf-beta-like gene expressed in the mouse node during gastrulation. *Nature* **361**, 543-547, doi:10.1038/361543a0 (1993).
21 Varlet, I., Collignon, J. & Robertson, E. J. nodal expression in the primitive endoderm is required for specification of the anterior axis during mouse gastrulation. *Development* **124**, 1033-1044 (1997).
22 Perea-Gomez, A. *et al.* Nodal antagonists in the anterior visceral endoderm prevent the formation of multiple primitive streaks. *Developmental Cell* **3**, 745-756, doi:10.1016/s1534-5807(02)00321-0 (2002).
23 Streit, A. *et al.* Chordin regulates primitive streak development and the stability of induced neural cells, but is not sufficient for neural induction in the chick embryo. *Development* **125**, 507-519 (1998).
24 Loebel, D. A. F., Watson, C. M., De Young, A. & Tam, P. P. L. Lineage choice and differentiation in mouse embryos and embryonic stem cells. *Developmental Biology* **264**, 1-14, doi:10.1016/s0012-1606(03)00390-7 (2003).
25 Kalluri, R. & Weinberg, R. A. The basics of epithelial-mesenchymal transition. *Journal of Clinical Investigation* **119**, 1420-1428, doi:10.1172/jci39104 (2009).
26 Grau, Y., Carteret, C. & Simpson, P. Mutations and chromosomal rearrangements affecting the expression of snail, a gene involved in embryonic patterning in drosophila-melanogaster. *Genetics* **108**, 347-360 (1984).
27 Cano, A. *et al.* The transcription factor Snail controls epithelial-mesenchymal transitions by repressing E-cadherin expression. *Nature Cell Biology* **2**, 76-83, doi:10.1038/35000025 (2000).
28 Ryan, K., Garrett, N., Mitchell, A. & Gurdon, J. B. Eomesodermin, a key early gene in Xenopus mesoderm differentiation. *Cell* **87**, 989-1000, doi:10.1016/s0092-8674(00)81794-8 (1996).
29 Arnold, S. J., Hofmann, U. K., Bikoff, E. K. & Robertson, E. J. Pivotal roles for eomesodermin during axis formation, epithelium-to-mesenchyme transition and endoderm specification in the mouse. *Development* **135**, 501-511, doi:10.1242/dev.014357 (2008).
30 Saga, Y., Kitajima, S. & Miyagawa-Tomita, S. Mesp1 expression is the earliest sign of cardiovascular development. *Trends in Cardiovascular Medicine* **10**, 345-352, doi:10.1016/s1050-1738(01)00069-x (2000).
31 Lindsley, R. C. *et al.* Mesp1 coordinately regulates cardiovascular fate restriction and epithelial-mesenchymal transition in differentiating ESCs. *Cell Stem Cell* **3**, 55-68, doi:10.1016/j.stem.2008.04.004 (2008).
32 Park, C., Kim, T. M. & Malik, A. B. Transcriptional Regulation of Endothelial Cell and Vascular Development. *Circulation Research* **112**, 1380-1400, doi:10.1161/circresaha.113.301078 (2013).
33 Marcelo, K. L., Goldie, L. C. & Hirschi, K. K. Regulation of Endothelial Cell Differentiation and Specification. *Circulation Research* **112**, 1272-1287, doi:10.1161/circresaha.113.300506 (2013).
34 (!!! INVALID CITATION !!!).
35 Ferkowicz, M. J. & Yoder, M. C. Blood island formation: longstanding observations and modern interpretations. *Experimental Hematology* **33**, 1041-1047, doi:10.1016/j.exphem.2005.06.006 (2005).
36 Medvinsky, A., Rybtsov, S. & Taoudi, S. Embryonic origin of the adult hematopoietic system: advances and questions. *Development* **138**, 1017-1031, doi:10.1242/dev.040998 (2011).
37 Ferguson, J. E., Kelley, R. W. & Patterson, C. Mechanisms of endothelial differentiation in embryonic vasculogenesis. *Arteriosclerosis Thrombosis and Vascular Biology* **25**, 2246-2254, doi:10.1161/01.atv.0000183609.55154.44 (2005).

38 Schmidt, A., Brixius, K. & Bloch, W. Endothelial precursor cell migration during vasculogenesis. *Circulation Research* **101**, 125-136, doi:10.1161/circresaha.107.148932 (2007).
39 Swift, M. R. & Weinstein, B. M. Arterial-Venous Specification During Development. *Circulation Research* **104**, 576-588, doi:10.1161/circresaha.108.188805 (2009).
40 Meadows, S. M., Ratliff, L. A., Singh, M. K., Epstein, J. A. & Cleaver, O. Resolution of Defective Dorsal Aortae Patterning in Sema3E-Deficient Mice Occurs Via Angiogenic Remodeling. *Developmental Dynamics* **242**, 580-590, doi:10.1002/dvdy.23949 (2013).
41 Coultas, L., Chawengsaksophak, K. & Rossant, J. Endothelial cells and VEGF in vascular development. *Nature* **438**, 937-945, doi:10.1038/nature04479 (2005).
42 Keck, P. J. *et al.* Vascular-permeability factor, an endothelial-cell mitogen related to pdgf. *Science* **246**, 1309-1312, doi:10.1126/science.2479987 (1989).
43 Olsson, A. K., Dimberg, A., Kreuger, J. & Claesson-Welsh, L. VEGF receptor signalling - in control of vascular function. *Nature Reviews Molecular Cell Biology* **7**, 359-371, doi:10.1038/nrm1911 (2006).
44 Fong, G. H., Zhang, L. Y., Bryce, D. M. & Peng, J. Increased hemangioblast commitment, not vascular disorganization, is the primary defect in flt-1 knock-out mice. *Development* **126**, 3015-3025 (1999).
45 Shalaby, F. *et al.* A requirement for Flk1 in primitive and definitive hematopoiesis and vasculogenesis. *Cell* **89**, 981-990, doi:10.1016/s0092-8674(00)80283-4 (1997).
46 Carmeliet, P. *et al.* Abnormal blood vessel development and lethality in embryos lacking a single VEGF allele. *Nature* **380**, 435-439, doi:10.1038/380435a0 (1996).
47 van Bueren, K. L. & Black, B. L. Regulation of endothelial and hematopoietic development by the ETS transcription factor Etv2. *Current Opinion in Hematology* **19**, 199-205, doi:10.1097/MOH.0b013e3283523e07 (2012).
48 Sharrocks, A. D. The ETS-domain transcription factor family. *Nature Reviews Molecular Cell Biology* **2**, 827-837, doi:10.1038/35099076 (2001).
49 De Haro, L. & Janknecht, R. Cloning of the murine ER71 gene (Etsrp71) and initial characterization of its promoter. *Genomics* **85**, 493-502, doi:10.1016/j.ygeno.2004.12.003 (2005).
50 Brown, T. A. & McKnight, S. L. Specificities of protein protein and protein DNA interaction of gabp-alpha and 2 newly defined ets-related proteins. *Genes & Development* **6**, 2502-2512, doi:10.1101/gad.6.12b.2502 (1992).
51 Sumanas, S. & Lin, S. Ets1-related protein is a key regulator of vasculogenesis in zebrafish. *Plos Biology* **4**, 60-69, doi:10.1371/journal.pbio.0040010 (2006).
52 Ferdous, A. *et al.* Nkx2-5 transactivates the Ets-related protein 71 gene and specifies an endothelial/endocardial fate in the developing embryo. *Proceedings of the National Academy of Sciences of the United States of America* **106**, 814-819, doi:10.1073/pnas.0807583106 (2009).
53 Kataoka, H. *et al.* Etv2/ER71 induces vascular mesoderm from Flk1(+)PDGFR alpha(+) primitive mesoderm. *Blood* **118**, 6975-6986, doi:10.1182/blood-2011-05-352658 (2011).
54 Salanga, M. C., Meadows, S. M., Myers, C. T. & Krieg, P. A. ETS Family Protein ETV2 Is Required for Initiation of the Endothelial Lineage but not the Hematopoietic Lineage in the Xenopus Embryo. *Developmental Dynamics* **239**, 1178-1187, doi:10.1002/dvdy.22277 (2010).
55 Hayashi, M. *et al.* Endothelialization and altered hematopoiesis by persistent Etv2 expression in mice. *Experimental Hematology* **40**, 738-750, doi:10.1016/j.exphem.2012.05.012 (2012).
56 Garciamartinez, V. & Schoenwolf, G. C. Primitive-streak origin of the cardiovascular-system in avian embryos. *Developmental Biology* **159**, 706-719, doi:10.1006/dbio.1993.1276 (1993).
57 Schoenwolf, G. C. & GarciaMartinez, V. Primitive-streak origin and state of commitment of cells of the cardiovascular system in avian and mammalian embryos. *Cellular & Molecular Biology Research* **41**, 233-240 (1995).

58 Abu-Issa, R. & Kirby, M. L. in *Annual Review of Cell and Developmental Biology* Vol. 23 *Annual Review of Cell and Developmental Biology* 45-68 (2007).
59 Davis, C. L. Development of the human heart from its first appearance to the stage found in embryos of twenty paired somites. *Contributions to Embryology* **19**, 247-U239 (1927).
60 Deruiter, M. C., Poelmann, R. E., Vanderplasdevries, I., Mentink, M. M. T. & Gittenbergerdegroot, A. C. The development of the myocardium and endocardium in mouse embryos - fusion of 2 heart tubes. *Anatomy and Embryology* **185**, 461-473 (1992).
61 Zaffran, S. & Frasch, M. Early signals in cardiac development. *Circulation Research* **91**, 457-469, doi:10.1161/01.res.0000034152.74523.a8 (2002).
62 High, F. A. & Epstein, J. A. The multifaceted role of Notch in cardiac development and disease. *Nature Reviews Genetics* **9**, 49-61, doi:10.1038/nrg2279 (2008).
63 Stalsber.H & Dehaas, R. L. Precardiac areas and formation of tubular heart in chick embryo. *Developmental Biology* **19**, 128-&, doi:10.1016/0012-1606(69)90052-9 (1969).
64 Bodmer, R. The gene tinman is required for specification of the heart and visceral muscles in drosophila. *Development* **118**, 719-729 (1993).
65 Evans, S. M. Vertebrate tinman homologues and cardiac differentiation. *Seminars in Cell & Developmental Biology* **10**, 73-83, doi:10.1006/scdb.1999.0282 (1999).
66 Lints, T. J., Parsons, L. M., Hartley, L., Lyons, I. & Harvey, R. P. Nkx-2.5 - a novel murine homeobox gene expressed in early heart progenitor cells and their myogenic descendants *Development* **119**, 969-969 (1993).
67 Lyons, I. *et al.* Myogenic and morphogenetic defects in the heart tubes of murine embryos lacking the homeo box gene nkx2-5. *Genes & Development* **9**, 1654-1666, doi:10.1101/gad.9.13.1654 (1995).
68 Tanaka, M. *et al.* Vertebrate homologs of tinman and bagpipe: Roles of the homeobox genes in cardiovascular development. *Developmental Genetics* **22**, 239-249, doi:10.1002/(sici)1520-6408(1998)22:3<239::aid-dvg6>3.3.co;2-g (1998).
69 Biben, C. & Harvey, R. P. Homeodomain factor Nkx2-5 controls left/right asymmetric expression of bHLH gene eHand during murine heart development. *Genes & Development* **11**, 1357-1369, doi:10.1101/gad.11.11.1357 (1997).
70 Zou, Y. M. *et al.* CARP, a cardiac ankyrin repeat protein, is downstream in the Nkx2-5 homeobox gene pathway. *Development* **124**, 793-804 (1997).
71 Tanaka, M., Schinke, M., Liao, H. S., Yamasaki, N. & Izumo, S. Nkx2.5 and nkx2.6, homologs of Drosophila tinman, are required for development of the pharynx. *Molecular and Cellular Biology* **21**, 4391-4398, doi:10.1128/mcb.21.13.4391-4398.2001 (2001).
72 Patient, R. K. & McGhee, J. D. The GATA family (vertebrates and invertebrates). *Current Opinion in Genetics & Development* **12**, 416-422, doi:10.1016/s0959-437x(02)00319-2 (2002).
73 Reiter, J. F. *et al.* Gata5 is required for the development of the heart and endoderm in zebrafish. *Genes & Development* **13**, 2983-2995, doi:10.1101/gad.13.22.2983 (1999).
74 Gove, C. *et al.* Over-expression of GATA-6 in Xenopus embryos blocks differentiation of heart precursors. *Embo Journal* **16**, 355-368, doi:10.1093/emboj/16.2.355 (1997).
75 Peterkin, T., Gibson, A. & Patient, R. GATA-6 maintains BMP-4 and Nkx2 expression during cardiomyocyte precursor maturation. *Embo Journal* **22**, 4260-4273, doi:10.1093/emboj/cdg400 (2003).
76 Morrisey, E. E., Ip, H. S., Lu, M. M. & Parmacek, M. S. GATA-6: A zinc finger transcription factor that is expressed in multiple cell lineages derived from lateral mesoderm. *Developmental Biology* **177**, 309-322, doi:10.1006/dbio.1996.0165 (1996).
77 Morrisey, E. E., Ip, H. S., Tang, Z. H., Lu, M. M. & Parmacek, M. S. GATA-5: A transcriptional activator expressed in a novel temporally and spatially-restricted pattern during embryonic development. *Developmental Biology* **183**, 21-36, doi:10.1006/dbio.1996.8485 (1997).

78 Molkentin, J. D., Lin, Q., Duncan, S. A. & Olson, E. N. Requirement of the transcription factor GATA4 for heart tube formation and ventral morphogenesis. *Genes & Development* **11**, 1061-1072, doi:10.1101/gad.11.8.1061 (1997).
79 Jiang, Y. M., Tarzami, S., Burch, J. B. E. & Evans, T. Common role for each of the cGATA-4/5/6 genes in the regulation of cardiac morphogenesis. *Developmental Genetics* **22**, 263-277, doi:10.1002/(sici)1520-6408(1998)22:3<263::aid-dvg8>3.0.co;2-4 (1998).
80 Merscher, S. *et al.* TBX1 is responsible for cardiovascular defects in Velo-Cardio-Facial/DiGeorge syndrome. *Cell* **104**, 619-629, doi:10.1016/s0092-8674(01)00247-1 (2001).
81 Bruneau, B. G. *et al.* A murine model of Holt-Oram syndrome defines roles of the T-box transcription factor Tbx5 in cardiogenesis and disease. *Cell* **106**, 709-721, doi:10.1016/s0092-8674(01)00493-7 (2001).
82 Chapman, D. L. *et al.* Expression of the T-box family genes, Tbx1-Tbx5, during early mouse development. *Developmental Dynamics* **206**, 379-390, doi:10.1002/(sici)1097-0177(199608)206:4<379::aid-aja4>3.0.co;2-f (1996).
83 Harris, I. S. & Black, B. L. Development of the Endocardium. *Pediatric Cardiology* **31**, 391-399, doi:10.1007/s00246-010-9642-8 (2010).
84 Stainier, D. Y. R., Weinstein, B. M., Detrich, H. W., Zon, L. I. & Fishman, M. C. Cloche, an early acting zebrafish gene, is required by both the endothelial and hematopoietic lineages. *Development* **121**, 3141-3150 (1995).
85 Czirok, A. & Little, C. D. Pattern formation during vasculogenesis. *Birth Defects Res. Part C-Embryo Today-Rev.* **96**, 153-162, doi:10.1002/bdrc.21010 (2012).
86 Piliszek, A., Kwon, G. S. & Hadjantonakis, A.-K. Ex utero culture and live imaging of mouse embryos. *Methods in molecular biology (Clifton, N.J.)* **770**, 243-257, doi:10.1007/978-1-61779-210-6_9 (2011).
87 Garcia, M. D., Udan, R. S., Hadjantonakis, A.-K. & Dickinson, M. E. Live imaging of mouse embryos. *Cold Spring Harbor protocols* **2011**, pdb.top104-pdb.top104, doi:10.1101/pdb.top104 (2011).
88 Yamanaka, Y., Tamplin, O. J., Beckers, A., Gossler, A. & Rossant, J. Live imaging and genetic analysis of mouse notochord formation reveals regional morphogenetic mechanisms. *Developmental Cell* **13**, 884-896, doi:10.1016/j.devcel.2007.10.016 (2007).
89 Roman, B. L. & Weinstein, B. M. Building the vertebrate vasculature: research is going swimmingly. *Bioessays* **22**, 882-893, doi:10.1002/1521-1878(200010)22:10<882::aid-bies3>3.0.co;2-j (2000).
90 Drake, C. J. & Fleming, P. A. Vasculogenesis in the day 6.5 to 9.5 mouse embryo. *Blood* **95**, 1671-1679 (2000).
91 Haar, J. L. & Ackerman, G. A. Phase and electron microscopic study of vasculogenesis and erythropoiesis in yolk sac of mouse. *Anatomical Record* **170**, 199-&, doi:10.1002/ar.1091700206 (1971).
92 Miquerol, L., Langille, B. L. & Nagy, A. Embryonic development is disrupted by modest increases in vascular endothelial growth factor gene expression. *Development* **127**, 3941-3946 (2000).
93 Fong, G. H., Rossant, J., Gertsenstein, M. & Breitman, M. L. ROLE OF THE FLT-1 RECEPTOR TYROSINE KINASE IN REGULATING THE ASSEMBLY OF VASCULAR ENDOTHELIUM. *Nature* **376**, 66-70, doi:10.1038/376066a0 (1995).
94 Shalaby, F. *et al.* Failure of blood-island formation and vasculogenesis in flk-1-deficient mice. *Nature* **376**, 62-66, doi:10.1038/376062a0 (1995).
95 Ema, M., Takahashi, S. & Rossant, J. Deletion of the selection cassette, but not cis-acting elements, in targeted Flk1-lacZ allele reveals Flk1 expression in multipotent mesodermal progenitors. *Blood* **107**, 111-117, doi:10.1182/blood-2005-05-1970 (2006).

96 Cheng, J. *et al.* Expression of vascular endothelial growth factor and receptor flk-1 in colon cancer liver metastases. *Journal of Hepato-Biliary-Pancreatic Surgery* **11**, 164-170, doi:10.1007/s00534-003-0883-2 (2004).
97 Pidgeon, G. P., Barr, M. P., Harmey, J. H., Foley, D. A. & Bouchier-Hayes, D. J. Vascular endothelial growth factor (VEGF) upregulates BCL-2 and inhibits apoptosis in human and murine mammary adenocarcinoma cells. *British Journal of Cancer* **85**, 273-278, doi:10.1054/bjoc.2001.1876 (2001).
98 Downs, K. M. & Davies, T. Staging of gastrulating mouse embryos by morphological landmarks in the dissecting microscope. *Development* **118**, 1255-1266 (1993).
99 Ishitobi, H. *et al.* Flk1-GFP BAC Tg Mice: An Animal Model for the Study of Blood Vessel Development. *Exp. Anim.* **59**, 615-622 (2010).
100 Risau, W., Flamme, I Vasculogenesis *Annual Review Of Cell And Developmental Biology* **11**, 73-91 (1995).
101 Yamaguchi, T. P., Dumont, D. J., Conlon, R. A., Breitman, M. L. & Rossant, J. Flk-1, an flt-related receptor tyrosine kinase is an early marker for endothelial-cell precursors. *Development* **118**, 489-498 (1993).
102 Strilic, B. *et al.* The Molecular Basis of Vascular Lumen Formation in the Developing Mouse Aorta. *Developmental Cell* **17**, 505-515, doi:10.1016/j.devcel.2009.08.011 (2009).
103 Yamashita, J. *et al.* Flk1-positive cells derived from embryonic stem cells serve as vascular progenitors. *Nature* **408**, 92-96, doi:10.1038/35040568 (2000).
104 Ema, M. *et al.* Combinatorial effects of Flk1 and Tal1 on vascular and hematopoietic development in the mouse. *Genes & Development* **17**, 380-393, doi:10.1101/gad.1049803 (2003).
105 Motoike, T., Markham, D. W., Rossant, J. & Sato, T. N. Evidence for novel fate of Flk1(+) progenitor: Contribution to muscle lineage. *Genesis* **35**, 153-159, doi:10.1002/gene.10175 (2003).
106 Moretti, A. *et al.* Multipotent embryonic Isl1(+) progenitor cells lead to cardiac, smooth muscle, and endothelial cell diversification. *Cell* **127**, 1151-1165, doi:10.1016/j.cell.2006.10.029 (2006).
107 Kattman, S. J., Huber, T. L. & Keller, G. M. Multipotent Flk-1(+) cardiovascular progenitor cells give rise to the cardiomyocyte, endothelial, and vascular smooth muscle lineages. *Developmental Cell* **11**, 723-732, doi:10.1016/j.devcel.2006.10.002 (2006).
108 Wilson, V., Manson, L., Skarnes, W. C. & Beddington, R. S. P. the t-gene is necessary for normal mesodermal morphogenetic cell movements during gastrulation. *Development* **121**, 877-886 (1995).
109 Fehling, H. J. *et al.* Tracking mesoderm induction and its specification to the hemangioblast during embryonic stem cell differentiation. *Development* **130**, 4217-4227, doi:10.1242/dev.00589 (2003).
110 Hattori, K. *et al.* Placental growth factor reconstitutes hematopoiesis by recruiting VEGFR1(+) stem cells from bone-marrow microenvironment. *Nat. Med.* **8**, 841-849, doi:10.1038/740 (2002).
111 Hahn, H. Experimentelle Studien über die Entstehung des Blutes und der ersten Geäße beim Hühnchen. *Anatomical Record* **33**, 153-170 (1908).
112 Klessinger, S. & Christ, B. Axial structures control laterality in the distribution pattern of endothelial cells. *Anat. Embryol.* **193**, 319-330 (1996).
113 Gerhardt, H. *et al.* VEGF guides angiogenic sprouting utilizing endothelial tip cell filopodia. *Journal of Cell Biology* **161**, 1163-1177, doi:10.1083/jcb.200302047 (2003).
114 Hiratsuka, S. *et al.* Vascular endothelial growth factor A (VEGF-A) is involved in guidance of VEGF receptor-positive cells to the anterior portion of early embryos. *Molecular and Cellular Biology* **25**, 355-363, doi:10.1128/mcb.25.355-363.2005 (2005).

115 de Almodovar, C. R. *et al.* VEGF Mediates Commissural Axon Chemoattraction through Its Receptor Flk1. *Neuron* **70**, 966-978, doi:10.1016/j.neuron.2011.04.014 (2011).
116 Rupp, P. A., Czirok, A. & Little, C. D. alpha v beta 3 integrin-dependent endothelial cell dynamics in vivo. *Development* **131**, 2887-2897, doi:10.1242/dev.01160 (2004).
117 Kamei, M. *et al.* Endothelial tubes assemble from intracellular vacuoles in vivo. *Nature* **442**, 453-456, doi:10.1038/nature04923 (2006).
118 van den Hoff, M. J. B., Kruithof, B. P. T., Moorman, A. F. M., Markwald, R. R. & Wessels, A. Formation of myocardium after the initial development of the linear heart tube. *Developmental Biology* **240**, 61-76, doi:10.1006/dbio.2001.0449 (2001).
119 Shimshek, D. R. *et al.* Codon-improved Cre recombinase (iCre) expression in the mouse. *Genesis* **32**, 19-26, doi:10.1002/gene.10023 (2002).